RESEARCH ARTICLE

Centralized Control Method for Voltage Coordination Challenges With OLTC and D-STATCOM in Smart Distribution Networks Based IoT Communication Protocol

AHMED Y. HATATA[1,2], **EMAN. O. HASAN**[1,3], **MOHAMMED A. ALGHASSAB**[1],
AND BISHOY E. SEDHOM[2], **(Member, IEEE)**
[1]Department of Electrical Engineering, College of Engineering, Shaqra University, Al-Dawadmi, Riyadh 11911, Saudi Arabia
[2]Electrical Engineering Department, Faculty of Engineering, Mansoura University, El-Mansoura, Mansoura 35516, Egypt
[3]North Delta Electricity Distribution Company (NDEDC), Mansoura 35516, Egypt

Corresponding author: Bishoy E. Sedhom (eng_bishoy90@mans.edu.eg)

ABSTRACT This paper proposes a coordination method for the voltage control devices based on optimal settings of the D-STATCOMs, on the load tap changer (OLTC) transformer and the distributed generations (DGs)-based renewable energy resources (RERs). The central controller is introduced to handle the active smart distribution network (SDN) problems to maintain the voltage profile within its permissible limits, minimize power losses in different operating conditions, and minimize the energy wastage from the distributed renewable energy resources. These problems are formulated as a multi-objective optimization problem. With increasing load demand and RERs in the distribution system, voltage coordination threatens real-time efficiency. In this research work, central controller-based Gorilla Troops optimization (GTO) algorithm is proposed to detect the optimum solutions for the voltage coordination problem. The load demand uncertainty and the stochastic nature of power generated from RERs (PV panels and wind turbines) are considered in the voltage coordination problem due to their significant effects on the operation and planning of the SDN. The proposed SDN has been represented based on the Internet of Things (IoT) communication protocol. It enhances the data and information transfer between the system-connected agents. A practical test system, NDEDC-24 bus radial distribution network from the North Delta Electrical Distribution Company and IEEE-33 node system are used to test and evaluate the proposed method. The results are compared with other well-known evolutionary methods. The proposed method obtains more accurate results than the other methods.

INDEX TERMS D-STATCOM, distribution network, Internet of Things, on-load tap changer, voltage coordination.

I. INTRODUCTION

The load-growing requirements have led to congestion in the contemporary electric grids. They consist of several stages of distribution, transmission, and generation systems [1]. The distribution systems supply the low-voltage consumers by converting the high voltage from the transmission networks.

The associate editor coordinating the review of this manuscript and approving it for publication was Renato Ferrero.

For distribution networks (DNs), the voltage profile is one of the most important parameters. DNs operators are responsible for maintaining consumers' voltage within its acceptable limits. The mitigation strategies of the voltage violation are used to ensure that the network bus voltages are always suppressed at the allowable values [1], [2], [3].

Several studies presented various techniques to remedy the voltage violation in the active DNs-connected distributed generations (DGs). The mitigation methods for

the voltage violation can be classified into; static transfer switch, reactive power control, demand-side management, on-load tap changer (OLTC) transformer, feeder enhancement, and energy storage systems [3]. The following sections present a brief literature review regarding voltage mitigation methods.

Power electronics-based compensation devices such as distribution static compensator (D-STATCOM) and static var compensation (SVC) have a fast response and large capacity of the reactive power injection [4]. D-STACOM devices, with their ability to control the power flow and voltage, can be a solution to mitigate voltage violation [5]. The optimization algorithms, such as bacterial foraging optimization algorithm, genetic algorithm (GA), fuzzy logic, and ant colony optimization approach, were used in previous researches to determine the optimal locations and ratings of D-STATCOMs in DNs for mitigating the voltage violation and reduce power losses [6], [7], [8]. A mixed-integer conic model was used to determine the solution of the optimal ratings and locations of the D-STATCOMs devices [9]. The discrete version sine-cosine algorithm was presented in [10] to obtain the optimum sizing and location of the D-STATCOM to minimize the operating costs in the DNs. The differential evolution algorithms were used to find the optimal location of D-STATCOM in the DNs [11], [12]. The impacts of reconfiguration on the optimal D-STATCOM placement problem were addressed in [11]. Reference [12] determined the D-STATCOM rating by injecting the optimal voltage phase angle at the optimal location. The forward–backward sweep load flow method was utilized to calculate the power flow and losses in DNs. It presented a D-STATCOM model to compensate for the reactive power and reduce power losses [12]. D-STATCOM's optimal placement and size problem was solved using the modified BAT algorithm to avoid the voltage violation problem [13]. The power system analysis toolbox was used to control the operating steps of the D-STATCOM module [14]. Moreover, it was applied to find the impacts of connecting the D-STATCOM on the system loading ability and voltage to satisfy the optimal quality of the system.

The OLTC regulates the voltage by varying the tapping of transformer windings while the transformer is under-loading. The voltages of the transformer secondary windings buses can be adjusted by optimally selecting the suitable tap position [15]. The electronic OLTC was utilized to maintain the load voltages within the permissible limits by simulating it using the MATLAB program [16]. The artificial neural network was used to control the electronic OLTC to maintain the voltage magnitudes at the load buses [17]. The OLTC and demand response (DR) were integrated to control the voltage in the unbalance DNs [18]. Also, particle swarm optimization (PSO) was applied to find the location and rating of OLTC settings and DR, respectively. However, relying on the OLTC alone to regulate the voltage may increase the customers' voltage near the transformers, especially for long radial feeders.

Integration of DGs-based renewable energy resources (RERs) with radial DNs has been studied in recent decades. As the installed DGs are not appropriately planned, technical issues such as system unbalance, voltage fluctuation, system unbalance, and overvoltage may have arisen. Furthermore, an increase in the voltage level of buses and power losses result from the load variations and the intermittent power generation of the RERs, such as PV and wind power [19], [20], [21]. The impact of several DG penetrations and concentrations levels on the long-term investment deferral of the DN was assessed in [22]. An approach was developed relayed on the amount that the network radial feeder currents were reduced by DG units [23]. Thus, proper DG allocations (size and location) into the radial DN are required to minimize these problems [24], [25]. Various studies analyzed the integration of the DGs in the DNs from many points of view. Various approaches associated with the stability problem related to the wide penetration of PV energy into the power system were studied [26]. The algorithms of the ramp-rate control were used with the energy storage system to decrease the power fluctuation to the electric network [27]. Reference [28] studied the technical problems, such as stability and frequency disturbances, and voltage limit violation, which is resulted from connecting high penetration of PV systems to the DNs. Reference [29] applied the dragonfly algorithm to determine the optimal allocation of the DGs. An improved wild horse optimization technique was applied to find the optimal location and size of the DGs to increase reliability, improve the voltage profile, and reduce the power losses in radial DNs [30]. A model for optimal wind turbine-based DGs location was presented in [31] by using the mixed integer linear programming in the smart grids considering the effect of OLTC and power factor control methods. An improved multi-objective PSO algorithm was introduced to obtain the optimum simultaneous DG units' sizing and location to improve system stability and voltage profile and reduce active power losses [32].

Many studies have combined more than one voltage control method to mitigate voltage violation and minimize power losses [33], [34], [35], [36]. The PSO algorithm was used to control the voltage as an auxiliary service with capacitors, DGs, and OLTC [33], [34], [35]. The capacitor bank and OLTC were used to control the voltage in the DNs in the presence of DGs [33]. These methods need appropriate coordination to perform their function well. Moreover, without appropriate coordination between the capacitors, DGs, and OLTC, many issues can arise, such as increasing the number of OLTCs switching operations, releasing the negative impacts of DG integrations, and increasing the voltage profile to exceed the permissible limits. The management between OLTC, DGs-based PV panels, and compensation devices was presented for controlling the voltage by using GA [37]. It was used to obtain the optimal setting of capacitors banks, DGs, and OLTC. The voltage-VAR Optimization algorithm was proposed to control the voltage in

unbalanced DN [15], [38], [39]. The DN was divided into control areas, each linked with DG, capacitor bank, and OLTC. The Mixed-integer quadratic programming model for Voltage/VAR control was introduced with two phases and various time ranges in the existence of DGs in DN [15], [38]. A coordination method was presented to maintain the voltage within its permissible limits and minimize the feeder losses [39]. It was based on finding the optimal coordination between OLTC, shunt capacitors, and DGs and determining the optimal location to install these controlling devices using the PSO technique.

Dealing with uncertainty is one of the important planning issues in power systems due to the dynamic variations of consumers' loads and/or the penetration of RERs. Therefore, an appropriate uncertainty management method is required to make accurate decisions for the penetration of the RERs in the DNs. An approach for power distribution voltage regulators in medium voltage distribution networks was presented in [40]. The deviation of solar and wind power generations from their predicted or scheduled values was presented in [41]. The solar radiation and the wind speed were simulated by a normal distribution and the Weibull-distributed, respectively. The artificial hummingbird algorithm was applied to determine the optimal location of wind turbines and PV panels in IEEE 33-bus and 94-bus test systems to minimize emissions, cost, and voltage deviation, and improve voltage stability, considering load demands, wind speed, and solar radiation uncertainties [42]. Considering the uncertain parameters results in more efficiency and accuracy of the models; however, it also increases the model's computing weights and complexity [43], [44].

The voltage control and management were performed using centralized and decentralized approaches. In the centralized methods, system data was collected from all buses and sent to the central control and management unit through communication links. Then the data was processed, and the command signals were sent back to the voltage control devices to regulate the system voltage within its nominal values [45]. It has many advantages, such as accessible to implementation, high controllability, low-cost, and real-time monitoring for all system parameters; also, the data is safeguarded in central units. Also, it can achieve the system's global objective and coordinate different devices simultaneously. Furthermore, it contains a memory that stores the different voltage violation scenarios and then can regulate the voltage reasonably based on the stored data [46], [47]. However, it suffered many disadvantages, such as a single failure point and a lack of flexibility and scalability. To enhance the performance of the centralized control and management schemes, high bandwidth communication is required for data and information exchange on a timely basis, and more redundancy can be added to the control and communication infrastructure [46]. On the other hand, each unit and device in the system was treated as standalone and controlled using its local data when the decentralized controllers were applied. The decentralized approach did not require communication links

as it was based on local measurement without full awareness of all the system data. The lack of coordination between devices made achieving the global objective difficult [47]. The implementation difficulty was higher and did not ensure optimal performance due to the lack of a global view of the system and the cooperation between the different system devices [48].

The Internet of things (IoT) has been recently integrated with conventional DNs to perform SDNs. The SDN included various smart objects such as smart meters, smart appliances, and sensors that were interconnected and communicated with each other for transferring data and information between these devices. IoT enabled the system to be monitored, improved the system performance, and enhanced real-time decision-making [49], [50]. It could be applied for controlling, monitoring, and protecting the smart substation equipments with low cost, high reliability, and human resources reduction [51]. It provided many features to the end users, such as accessibility, scalability, and mobility, ensuring data storage and processing at a low cost [52]. Enhancing the system voltage regulation with power management using central control based on a wireless flow sensor was reported in [53]. In [54], the voltage was regulated in SDNs using a smart inverter, data distribution service (DDS), and IoT-based communication platform. Local and coordinated control was applied to mitigate the voltage violation in the DN with high penetration of the DGs [54]. The optimal allocation and operation of the flexible AC transmission systems (FACTs) in the cyber-physical DN-based IoT communication platform was discussed in [55].

From the above literature review, the research gap can be summarized as follows;

1- The centralized control for coordinating different voltage regulation devices, such as OLTC and STATCOM, in the presence of DGs to achieve a global objective is not investigated.
2- The use of IoT-based communication channels for SDNs is not considered.
3- The multi-objective metaheuristic optimization method for the voltage coordination problem to minimize the power losses, DGs' energy wastage, and a number of OLTC-tap operations while investigating the effect of system uncertainties is not considered.

This paper applies a new multi-objective metaheuristic optimization method called Gorilla Troops Optimizer (GTO) algorithm to solve the optimal voltage coordination problem in SDNs. The SDNs are performed for data and information transfer capabilities, system monitoring, and supervision processes. The SDN is designed based on IoT technology that can connect all the system agents in the network. Four layers are proposed for the SDN architecture: physical, communication, processing, and cyber. Long-range wide area network (LoRaWAN) technology is applied as a wireless communication channel. A central controller for the voltage coordination between the D-STATCOM, OLTC, and DGs in

the SDN is applied in this paper. The proposed method is used to find the optimal ratings of the DGs, the D-STATCOMs, and the OLTC-operating tap in the SDNs. Solving the voltage coordination problem aims to minimize the energy wastages from the DGs-based RERs, the active power losses in the lines, and the number of tap operations of the OLTC. This paper uses two types of DGs: PV panels and wind turbines. Also, the uncertainty model of the solar radiations and the wind speed is considered in solving the voltage coordination problem. A practical test system, NDEDC-24 bus radial distribution network from the North Delta Electrical Distribution Company, and a modified IEEE-33 node system are used to test and evaluate the proposed method. The novelty of the paper can be summarized as follows:

1. Proposing a central controller for real-time voltage coordination between the SDN's DGs, OLTC, and D-STATCOM.
2. Designing SDN based on IoT technology with four layers for enhancing the data and information transferring capabilities and performing the voltage regulation.
3. A new multi-objective metaheuristic optimization method based on the Gorilla Troops Optimizer is applied to solve the voltage control coordination problem.
4. The objectives of the proposed voltage coordination method are to minimize the power losses and the energy wastage of the DGs (PV and wind). Also, it determines the optimal number of OLTC-tap operations.
5. The coordination method is performed in practice DN with hourly load demand variations. Also, the uncertainty of solar radiation and wind speed is considered.

This paper is structured as follows: section II describes the voltage violation problem in the DNs. The voltage violation mitigation strategies are explained in section III. Also, the uncertainty models of solar radiation and wind speed are illustrated in the same section. Section IV presents the proposed IoT-based system architecture for the SDNs. Section V consists of the voltage coordination problem's objective function and constraints. The proposed GTO method is explained, and the applied steps of the method to find the optimal coordination of the voltage control problem is explained in section VI. The test system and the simulation results of the GTO-based coordination of voltage control are illustrated in sections VII and VIII. Finally, the conclusions of the paper are specified in section IX.

II. VOLTAGE VIOLATION PROBLEM IN THE DISTRIBUTION SYSTEM

Voltage violation is one of the most important problems that occur in DNs. The main source of this violation is domestic consumers and industrial loads. In conventional DN, the normal power flow direction is from the distribution transformer toward the load. The voltage is adjusted over the nominal voltage at the distribution transformer to recompense the voltage drop in the feeder. Therefore, the voltage decreases as we move away from the distribution transformers along

the feeder, and the lowest voltage occurs at the end of the line at the consumers. The case is complex in practice due to the unbalanced DN along the feeders [3]. The medium voltage DNs in North Delta Electrical Distribution Company (NDEDC) are operated on 11 kV. While the nominal low voltage at the consumers is 380V, and the under-voltage is considered if the voltage becomes lower than 340V. This under-voltage depends on the feeder impedance, load currents along the feeder, vicinity to voltage-controlling equipment, and the load power factor. The NDEDC generally uses the off-load tap changers transformers to maintain the violation in voltages. So, the voltage of secondary windings of the distribution transformer is usually set higher than the nominal voltages to recompense the feeder voltage drops.

DG integration in the DNs of the NDEDC has grown in the last decade. Most DGs-based RERs are linked to the DNs via power electronic converters. The distributed PV with a power domain from 1 kVA to 50 kVA can cause voltage violations of the low-voltage DNs [56]. The power generated from the DGs reduces the power taken from the grid, and the load voltage depends on the DGs' produced power. In case of high penetration of DG power, the power flow inverses its direction to flow from the load buses to the distribution transformers. Therefore, the voltage magnitudes of the load buses will be greater than the distribution transformer depending on the power flow rate; also, the load voltage magnitude may be exceeded the permissible limits [57]. The long-term and short-term variations of the weather will affect the power produced by the DGs (Wind and PV sources); consequently, the voltage drop and power flow will change [58], [59]. The long-term variations are seasonal ambient temperature, wind speed, and sunshine through summer and winter. While the short-term variations include events such as solar radiation changes due to the clouds and wind speed changes during the day. Therefore, voltage fluctuation is a catastrophic problem caused by heavy loading or installing many DG types. They added additional challenges to the distribution system operators.

III. VOLTAGE-VIOLATION MITIGATION STRATEGIES

The load variations at consumers affect the voltage control and the DGs management in the DNs. Many strategies, such as shunt, series compensation, and OLTC, are used to solve the problem of voltage violations in DNs. In this paper, a combination of three different strategies is considered to regulate the voltage and minimize the power losses, the number of tap operations of OLTC, and the energy wastage from the distributed RERs.

A. ON LOAD TAP CHANGER MODELING

The tap changer of the transformer can be used as a booster transformer. It is one of the main strategies used to regulate the voltage in electrical networks [59]. The transformer's multiple taps, which can be On/Off taps, are used in the electric network to compensate for the voltage. By moving the taps from one position to another, the turns ratio of the
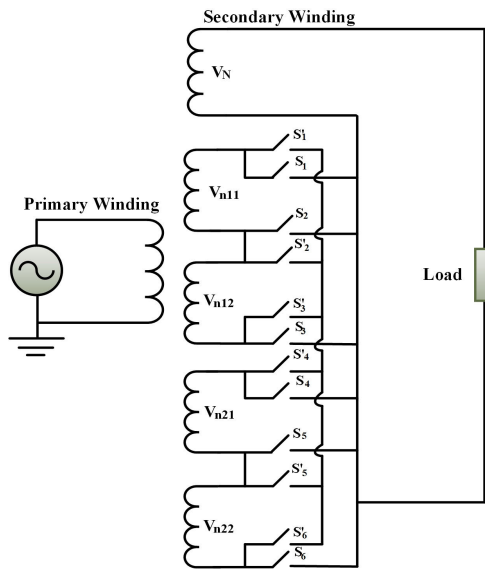
FIGURE 1. Transformer model including tap-changer winding and their switches.

transformer will be changed, and the terminal voltage also. The construction of the electronic OLTC is illustrated in Fig.1. It can be installed on either the low or medium-voltage side of the transformer. This paper studies the impact of the OLTC on voltage violation mitigation and line loss reduction. In normal conditions, the tap position is put at a nominal value. Increasing the tap position in the primary leads to a decrease in the secondary voltage. However, lowering the tap position leads to an increase in the voltage. The optimal configuration of the OLTC shown in Fig. 1 is used for the proposed control method.

To determine the voltage for each tap winding, Eqs. (1) and (2) should be satisfied [60].

$$V_{n11} = V_{step} \tag{1}$$
$$V_{n12} = 2V_{step} \tag{2}$$

The maximum realizable voltage, N_v, can be determined by;

$$N_v = n^2 - n + 1 \tag{3}$$

As a general form, the voltage for each tap winding can be expressed by [17],

$$V_{nj1} = N_v^{j-1} V_{step} \tag{4}$$
$$V_{nj2} = 2 \times N_v^{j-1} V_{step} \tag{5}$$

where V_{nj1} is the voltages of the tap winding, and V_{step} is the achievable voltage step. $j = 1, 2, \ldots$ total number of taps.

For example, if the number of taps is 3 for each tap winding, therefore, $N_v = 7$, $V_{nj1} = 7^{j-1} V_{step}$, and $V_{nj2} = 2 \times 7^{j-1} V_{step}$

B. D-STATCOM MODELING
D-STATCOM is a compensation device used to absorb or inject the reactive and active currents at a point of common
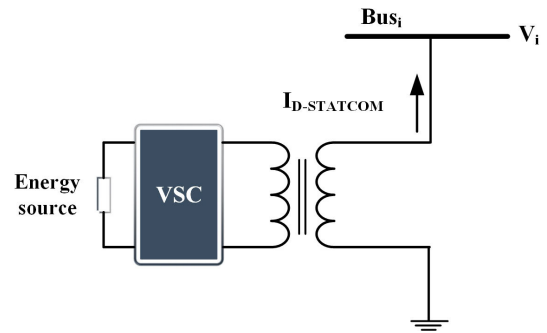
coupling (PCC) connection, respectively [60]. It can regulate the voltage of its bus and improve the power factor. The current can be generated/absorbed by changing the switch with a control strategy based on the voltage of the buses. The D-STATCOM typically injects a suitable compensating current to the PCC in steady-state operation. Thus, the voltage at the load bus controlled by the D-STATCOM will be raised near the nominal or a given value [61]. In general, D-STATCOM can interchange the reactive and active power simultaneously. In this study, the DSTATCOM is utilized for reactive power interchange. Figure 2 illustrates a bus in a DN equipped with a D-STATCOM. The D-STATCOM reactive power is determined by;

FIGURE 2. D-STATCOM connected to the bus i^{th} in DN.

$$jQ_{DS} = V_{i,new} I_{DS}^* \tag{6}$$

where $V_{i,new}$ is the voltage of the bus i^{th} after the compensation by D-STATCOM, I_{DS} is the D-STATCOM injected current, and $*$ denotes the conjugate of a complex variable, $V_{i,new} \angle \emptyset_{new}$.

C. DG MODELING
This paper's hybrid renewable energy system model depends on wind turbines and photovoltaic panels. These sources should be modeled as described in the following subsections.

1) WIND POWER SOURCE
The wind is caused by the rapid movement of hot air caused by solar energy. The wind turbine converts the kinetic energy in the wind to electric energy through a double-fed induction generator (DFIG). The wind turbine's electric energy depends on the wind speed and pitch angle [62]. The power produced by the wind turbine can be calculated by,

$$P_w = \begin{cases} 0 & 0 \leq v_{wind} \leq v_{in} \\ \rho A \frac{1}{2} v_{wind}^3 C_p & v_{in} \leq v_{wind} \leq v_r \\ P_{wr} & v_r \leq v_{wind} \leq v_0 \\ 0 & v_0 \leq v_{wind} \end{cases} \tag{7}$$

where, P_{wr} is the wind turbine-rated power, C_p is wind turbine coefficient, A is the wind turbine swept area, ρ is the air density coefficient, and v_{wind} is the wind speed. The v_{in}, v_0,

and v_r are the cut-in, cut-out, and rated wind turbine speed, respectively.

Determining the appropriate statistical model that represents the uncertain variables in the system is one of the most important planning steps. Due to its volatile nature, the wind speed is not fixed during the planning time; therefore, the output power from the wind turbine will not be a constant value over time. Statistical models of wind speed do not follow the normal distribution. Many researchers study the wind speed model as two parameters by Weibull distribution networks [63], [64], [65]. This model is helpful in long-term and short-term studies. The Weibull probability distribution function (PDF) is expressed by [64] and [65],

$$f(v) = \frac{h}{c} \left(\frac{v_{wind}}{c}\right)^{(h-1)} exp\left(-\frac{v_{wind}}{c}\right)^h \tag{8}$$

where, h and c are the shape and scale parameters of Weibull distribution, respectively. In this paper, the wind speed data is acquired from the daily wind speed. The wind turbine-generated power is dependent on the wind speed.

2) PV MODEL
Climatic conditions such as ambient temperature, clouds, and solar irradiance highly affect the PV panels' power output. In this paper, the power generated from the PV panels is calculated by using a simple model. This model uses the ambient temperature and the solar irradiation every hour as inputs. The power generated by the PV panels is given by the equation [62]:

$$P_{PV} = \eta A \left[1 - 0.005 \left(T_C - T_r\right)\right] G \tag{9}$$

where η is the conversion efficiency, A is the PV panels area, T_C is the cell temperature of PV, T_r is the reference temperature of PV, and G is the solar irradiation. The conversion efficiency of the PV panel is constant depending on the type of PV. The PV cell temperature, T_C, can be determined by,

$$T_C = T_a + \left(\frac{T_r - 20°C}{800}\right) G \tag{10}$$

where, T_a is the ambient temperature. It can be observed from (9) and (10) that the PV output power mainly depends on solar irradiation and ambient temperature.

The common parameters used to model the PV output uncertainty are humidity, air temperature, sky key index (sunny, cloudy, and clear), and solar radiation. The normal PDF, formulated in (11), models the air temperature and the solar radiation uncertainty. The normal distribution PDF for air temperature, and radiation, G, are calculated by [66]:

$$f(G) = \frac{1}{\sqrt{(2\pi)}\,\sigma_i} * exp\left[\left|-\frac{(G-\mu)^2}{2\sigma^2}\right|\right] \tag{11}$$

where σ and μ are the standard deviation and mean of forecasted radiation and air temperature, respectively. In each case, random solar radiation and air temperature are produced

each hourly. So, the output of PV power is determined by the following;

$$P_{pv} = P_{STC} * \frac{G}{G_{STC}} \lceil 1 + K(T_C + T_r\rceil \tag{12}$$

where K is the coefficient of maximum power temperature, P_{STC} is the rated power of PV, and G_{STC} is the standard radiation (1000 W/m^2).

IV. PROPOSED IoT-BASED SYSTEM ARCHITECTURE FOR SMART DISTRIBUTION NETWORK
In this section, the proposed smart distribution network (SDN) has been represented. The SDN consists of DGs, battery storage systems, D-STATCOMs, and OLTCs. The central controller is designed to regulate the SDN voltage using a coordination strategy between the DGs, OLTC, and D-STATCOM. It connected with all SDN agents with a communication channel for data monitoring, collecting, and reporting. Also, it enables the sending/receiving of the control signals between the central controller and all system smart agents. The communication channel is based on IoT technology that enables all physical agents in the SDN to receive, send, and share information among each other and between the agents and the central control unit. Also, it transfers the static agents into smart agents using their prevalent technologies as pervading computing, embedded systems, and communication technologies. All power-generating units, DGs, loads, and voltage-regulating devices are integrated into this platform.

According to the standard IEC 61850, the data distribution service (DDS) is applied as a messaging protocol. It is applied for the data and information collaboration middleware among the SDN's agents. It is used with the SDN to enhance its capability to easily share and communicate data between networks, devices, and components securely and efficiently. Also, it enables real-time communication, provides low data latency access, achieves high performance, enhances reliability and dependability, and ensures data exchange scalability. It enables standard application programming interfaces for C, C++, Java, and .Net to enhance multiple applications' integration. The voltage regulation process can be applied using IEEE 802.11n WLAN or Ethernet with the IEC 61850. It provides the appropriate sharing of the data and information between the SDN agents, D-STATCOM, OLTCs, and the central controller.

In this paper, the simulation implementation is achieved using the real-time innovation (RTI), Connext connectivity framework custom-built in MATLAB classes and DDS simulation blocks. These blocks are added to the simulated model to enable the model to communicate with other DDS members. In the simulation, the MATLAB/Simulink® coder produces C/C++ code from the model, and the generated code from the DDS blocks conforms to the RTI Connext DDS. Then the code is compiled and executed on the platform supported by RTI Connext DDS or RTI Connext Micro DDS framework.

The proposed SDN architecture comprises four layers, the physical layer, the communication layer, the processing layer, and the cyber layer.

A. PHYSICAL LAYER

The physical layer integrates all the system smart agents like; DGs, OLTCs, D-STATCOMs, loads, and buses for data collecting and monitoring. This layer contains sensors and measuring devices at every node in the SDN. The main purpose of these sensors is to measure the system voltage at each bus, the taps of the OLTCs, output power from each DG, stochastic input parameters of each DG, and D-STATCOM setting. It provides the central controller with the required data for achieving its goal.

B. COMMUNICATION LAYER

In this layer, the IoT-based communication platform is designed. It is the intermittent layer between the agents and the processing layer. It enables the measured data to transfer between these two layers in a secure channel. Two communication networks have been used: neighborhood area network (NAN) and wide area network (WAN). Long-range wide area network (LoRaWAN) technology is applied in this paper as a wireless communication channel. It can communicate with a long-range, low-power wide area network (LPWANs). It is easy to implement, has convenient coverage capabilities, ensures energy efficiency, enhances indoor penetration, and enables bidirectional connectivity for various IoT-based applications [67].

C. PROCESSING LAYER

In this layer, the measured data from the sensors in the SDN is processed using powerful processors. It performs the intended application to the collected data to enhance the system control function. It regulates the system voltage by indicating the DG sizing and localization, convenient tapping setting of the OLTC, and correct D-STATCOM designing. Also, it can deal with system uncertainties by ensuring the controller's ability to mitigate the effect of the stochastic DGs and load parameters. The control signals are sent to the SDN's agents via the LoRaWAN communication channel to regulate the DN's voltage within its acceptable limits.

D. CYBER LAYER

After the measured data is processed, the measured data are stored using middleware software which communicates the system agents and processed data with the storage servers. This layer is designed to be a cloud-based layer. It enhances the database's low sever and investment cost and provides the security and flexibility issues for the measured and processed data.

V. PROPOSED OPTIMAL VOLTAGE COORDINATION STRATEGY

This paper proposes a control strategy for voltage coordination between OLTC, D-STATCOM, and multiple combined DGs (wind and PV) in the SDN. The objectives of the coordination strategy are to improve the voltage profile, reduce the active power losses, the number of tap operations (TOs) of the OLTC, and DGs energy wastage (EW) due to the load changing during a day. The purpose of solving the coordination problem is to detect the optimal setting of the OLTC, D-STATCOM, and the multiple combined DGs (wind and PV) in the SDN. These settings are DG output power, the number of taps of the OLTC transformer, and the reactive power of the D-STATCOM. The objective function and the constraints of the coordination problem are represented in the following sections.

A. OBJECTIVE FUNCTION

The objective of implementing the proposed optimization algorithm is to minimize the Objective Function (OF), which is composed of minimizing the total power losses, TPL, the wind and PV energy waste (EW), and the number of tap operations (TOs) of the OLTC transformer during a time as will be illustrated in the following subsections.

1) TOTAL ACTIVE POWER LOSSES

The active power losses in the DNs are the major section of the power system losses. The objective of the total active power loss minimization, F1, is calculated using the power flow equations. The TPL is determined as the difference between the total power generated and the total load over a defined time horizon T so that it can be computed by,

$$F_1 = TP_L = \sum_{t=0}^{T} \left(\sum_{i=1}^{n_g} P_{g,t} - \sum_{i=1}^{n_d} P_{d,t} \right) \quad (13)$$

where $P_{d,t}$ and $P_{g,t}$ are the active power demand and generation at time t for each system bus i^{th}, respectively. n_d is the number of load buses and n_g is the number of generation buses.

2) TOTAL NUMBER OF TAP OPERATIONS

In DNs, the load continuously varies, so OLTC works many times in a given time. This reduces the service life of the OLTC transformer and thus increases the costs. In this paper, the proposed method is designed and implemented to reduce the number of TOs. So, the second term of the objective function is to minimize the total number of the TOs as,

$$F_2 = TO = \sum_{t=0}^{T} \left(\sum_{p=1}^{P} \left(|T_{p,t+1} - T_{p,t}| \right) \right) \quad (14)$$

where P is the total number of OLTCs tap positions and $T_{p,t}$ and $T_{p,t+1}$ are the tap position of OLTC at time step t and $t+1$, respectively. All tap changes over any two consecutive time steps over a defined time horizon T are arranged in F_2.

3) DGs POWER CURTAILMENT

The DGs energy wastage (Power Curtailment (PC)) is the difference between the total generated power from DGs (wind

and PV) and the total DGs available power at each time periods t. This value is always positive and should be reduced to full DG power capacity. Maximizing the injected DG power at some nodes may increase bus voltages and power losses. The DG power curtailment can be expressed by,

$$F_3 = PC = \sum_{t=0}^{T} \left(\sum_{dg=1}^{n_{dg}} \left(P_{dg,t}^{avl} - P_{dg,t}^{g} \right) \right) \quad (15)$$

where n_{dg} is the total number of DGs (Wind and PV). $P_{dg,t}^{avl}$ and $P_{dg,t}^{a}$ are the available and generated power from the DG at time t.

The summation method with weighted factors is used in this study to determine the gross OF that considers the minimization of both the TPL, TOs of OLTC, and PC of DGs for a defined time horizon T. Hence, the OF can finally be expressed by,

$$OF = min \left(\omega_1 * TP_L + \omega_2 * OT + \omega_3 * PC \right) \quad (16)$$

where ω_1, ω_2 and ω_3 are the weight factors. The objective function, OF, is a multi-objective function weighted with the summation of ω_1, ω_2, and ω_3. Increasing the weight ω_1 will improve the minimization of the total power losses over the total number of TO of the OLTC and PC of the DGs and vice versa. Therefore, the values of the weighted factors must be selected to satisfy the required balance between the total power losses, the number of TO of the OLTC, and the PC of the DGs. The best values of the weighted factors; ω_1, ω_2, and ω_3 depend on the feeder topologies, location and types of the DG, locations of OLTCs, and location of the compensation devices, so it varies from one feeder to another. Furthermore, these values may vary according to the engineer's concerns. So, the values of the weight factors ω_1, ω_2, and ω_3 are determined according to the relative viability and significance of each objective and satisfy equation (17). The weight factors ω_1, ω_2, and ω_3 are subjected to,

$$\sum_{i=1}^{3} \omega_i = 1 \quad \omega_i \in [0, 1] \quad (17)$$

In this paper, many combinations of the weighted factors are evaluated by applying them to the test system. Finally, best one is used to obtain the OF. For this analysis, the power losses have a higher weight (0.45) since it is important for distribution system. The DGs energy wastage (Power Curtailment (PC)) has the second major value (0.35) since it is important in the applications of the DGs. The number of tap operations of the OLTC receives a weight of (0.2), owing to the low number of OLTCs in the distribution system.

B. PROBLEM CONSTRAINTS

The OF in (16) is subjected to numerous constraints for the various variables; TPL, TO, and PC. These constraints are presented as follows;

1) POWER FLOW BALANCE

The balance of active and reactive power constraints equations are illustrated in (18) and (19),

$$P_{Gi} - P_{Di} = V_i \sum_{j=1}^{n_i} V_j (G_{ij} \cos (\theta_{ij})$$
$$+ B_{ij} sin(\theta_{ij})) \quad \text{for (i = 1...N)} \quad (18)$$

$$Q_{Gi} - Q_{Di} = V_i \sum_{j=1}^{n_i} V_j (G_{ij} \cos (\theta_{ij})$$
$$- B_{ij} sin(\theta_{ij})) \quad \text{for (i = 1...N)} \quad (19)$$

where P_{Di} and Q_{Di} are the active and reactive demand power at i^{th} bus, respectively. P_{Gi} and Q_{Gi} and are the active and reactive power generation at i^{th} bus, respectively. G_{ij} and B_{ij} are the conductance and susceptance of the line between i^{th} and j^{th} bus, respectively. θ_{ij} is the phasor voltage angle difference between bus i^{th} and j^{th}.

2) DISTRIBUTED GENERATION LIMITS

The injected power into the DN by DGs should be within maximum and minimum values as given in (20); also, the voltage magnitude limits of DG buses is defined by (21).

$$P_{DGi}^{min} \leq P_{DGi} \leq P_{DGi}^{max} \quad (20)$$
$$V_{DGi}^{min} \leq V_{DGi} \leq V_{DGi}^{max} \quad (21)$$

where P_{DGi}, P_{DGi}^{min}, and P_{DGi}^{max} are the generated, minimum, and maximum active power of DG at i^{th} bus, respectively. Q_{DGi}, Q_{DGi}^{min}, and Q_{DGi}^{max} are the generated, minimum, and maximum reactive power of DG at i^{th} bus, respectively. V_{DGi} is the set point of DG bus voltage. V_{DGi}^{max}, and V_{DGi}^{min} are the maximum and minimum limits of DG bus voltage, respectively.

3) BUS VOLTAGE LIMITS

The bus voltage magnitudes are to be maintained to the acceptable operating limits throughout the optimization process, as follows;

$$V_i^{min} \leq V_i \leq V_i^{max} \quad (22)$$

where V_i^{max} is the upper value of the voltage limit, and V_i^{min} is the lower value of the voltage limit, and V_i is the root mean square value of the ith bus voltage.

4) D-STACOM CONSTRAINTS

To avoid overcompensation, the injected reactive power from the D-STATCOMs should be equal to or less than the demand reactive power given in (23).

$$Q_{DST}(i) \leq Q_D(i) \quad (23)$$

where Q_D is the demand reactive power and Q_{DST} is the injected reactive power from the D-STATCOMs.
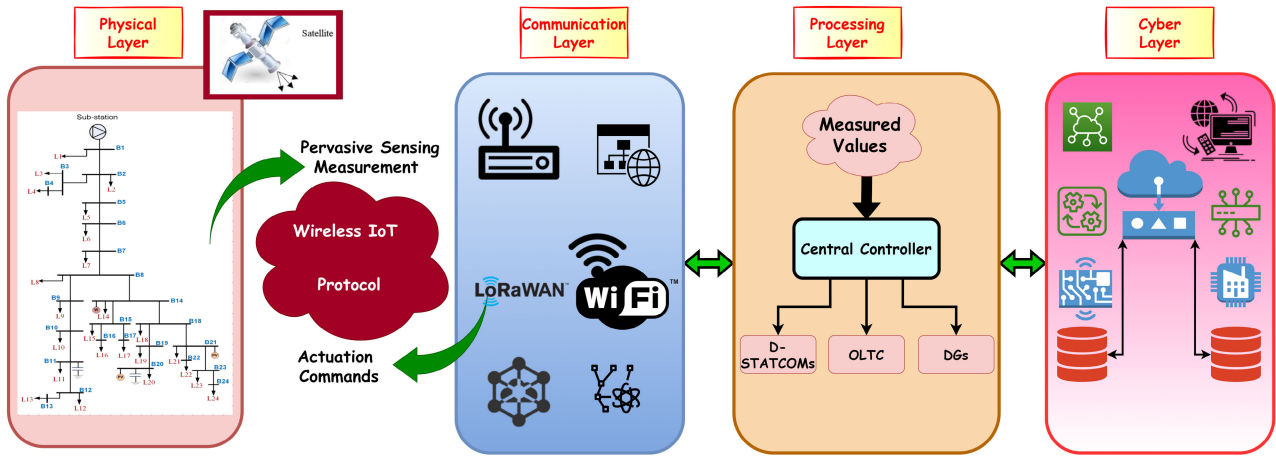
FIGURE 3. Proposed system architecture-based IoT Platform.

5) OLTC CONSTRAINTS

The voltage of the feeder feeding point can be changed using the OLTC to regulate the voltage magnitude over the feeder. It can adjust the magnitude of voltage within the range of rated voltage. The number of tap positions has a specific number of steps.

$$T_x^L \leq T_x \leq T_x^U \qquad (24)$$

where T_x is tap position of xth OLTC transformer. T_x^L and T_x^U are the lower and upper values of the tap position, respectively.

VI. GORILLA TROOPS OPTIMIZATION ALGORITHM (GTO)

Recently, natural-based metaheuristics techniques have become one of the most used techniques to solve engineering problems. This is due to the advantages of these techniques. They perform better than the local search techniques, do not need derivation function information, and are simple and easy in construction and implementation [68], [69]. Most of these techniques depend on the simulation of biological phenomena such as the behaviors of insects, swarms, plants, and animals. This paper uses a new technique called Gorilla Troops Optimizer (GTO), a naturally inspired metaheuristics technique that mimics the gorilla troop's group behavior.

The GTO consists of five stages to carry out the exploration and exploitation operations. The exploration phase is performed in three stages: immigration to known locations, immigration to unexplored locations, and going to other gorillas. These stages improve the efficiency and ability of the GTO algorithm searchability for the various optimization fields. Also, they help in achieving more balance between exploration and exploitation. On the other hand, the exploitations phase is performed in two stages: contesting for adult females and going behind the silverback (SB) [69]. Figure 4 illustrates the different phases of the GTO algorithm.
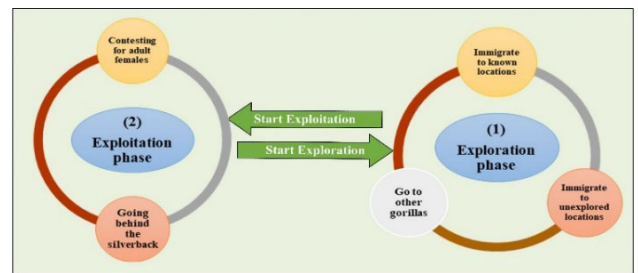

FIGURE 4. GTO exploitation and exploration phases.

A. EXPLORATION PHASE

As previously explained, the exploration phase consists of three operators according to the gorillas' group's lifestyle. So, all gorillas can consider as candidate solutions in the GTO algorithm, and the SB is the best optimum solution in each step. To select the appropriate operator of the three exploration operators, three conditions should be tested depending on the random variable, R. The operator, "immigration to known locations," is selected when R is smaller than a pre-describe value called P. While the second operator, "going to other gorillas," is selected if R is greater or equal to 0.5. Finally, the third operator, "immigration to unexplored locations," if R becomes smaller than 0.5. Eq. (25) modeled the selection mechanism of the three operators [69], [70].

$$
GL(t+1)
$$
$$
= \begin{cases} (UL - LL)\,rand_1 + LL & R < P \\ (rand_2 - C)\,L_r(t) + K \times H & R \geq 0.5 \\ L(i) - K\,(K\,(L(t) - GL_r(t)) \\ \quad + rand_3\,(L(t) - GL_r(t))), & R < 0.5 \end{cases} \qquad (25)
$$

where L_r is a randomly selected gorilla from the group. $GL(t)$ and $GL(t+1)$ are the candidate solutions of gorilla locations for iteration (t) and $(t+1)$, respectively. $rand_1$, $rand_2$, and $rand_3$ are random numbers in the range [0, 1]. LL and UL are the lower and upper limits of the variables. H, C,

and K are parameters that are calculated by,

$$C = (\cos(2 \times rand_4) + 1) \times \left(1 - \frac{t}{t_{max}}\right) \quad (26)$$

$$K = C \times l \quad (27)$$

$$H = Z \times L(t) \quad (28)$$

where Z, l, and $rand_4$ are random numbers in the range $[-C, C]$, $[-1, 1]$, and $[0, 1]$, respectively. t_{max} and t are the maximum and current iterations, respectively. The simulation of the SB leadership can be demonstrated by (28). The fitness value for all GL solutions can be determined at the end of the exploration phase, and if this fitness value is smaller than the $L(t)$ then it will be replaced with $GL(t)$. So, the SB can be assigned as the best-selected solution in this phase.

B. EXPLOITATION PHASE
Two operators can be implemented in this phase for optimization: contesting for adult females and going behind the SB. To select the appropriate operator in this phase, the C parameter is used. If C is equal to or greater than a pre-described parameter W, the first operator, "going behind the SB," is applied. However, the operator "contesting for adult females" is applied if C is smaller than W [69], [70].

The SB is strong and young for the recently created gorillas' group, and the gorillas in the group obey their orders. This operator is applied in the case of C greater than or equal to W and can be modeled by (29).

$$GL(t+1) = K \times M \times (L(t) - L_{SB}) + L(t) \quad (29)$$

$$M = \left(\left|\frac{1}{N}\sum_{i=1}^{N} GL_i(t)\right|^g\right)^{\frac{1}{g}} \quad (30)$$

$$g = 2^K \quad (31)$$

where N is the number of gorillas and L_{SB} is the best location in the SB. When young male gorillas grow up to adulthood, they start to compete with other young gorillas to extend their sphere of influence in choosing adult females. So, W is greater than the C parameter, and this operator can be simulated by;

$$GL(i) = X_{SB} - (2 \times rand_5 - 1) \times (X_{sb} - L(t)) \times \beta \times E \quad (32)$$

$$E = \begin{cases} N_1 & R \geq 0.5 \\ N_2 & R < 0.5 \end{cases} \quad (33)$$

where, E is the effect of violence on the dimensions of solutions. $rand_5$ is random numbers in the range $[0, 1]$. The fitness value for all GL solutions can be determined at the end of the exploration phase, and if this fitness value is smaller than the $L(t)$ then it will be replaced with $GL(t)$. So, the SB can be assigned as the best-selected solution in this phase.

C. OPTIMAL COORDINATION OF VOLTAGE CONTROL BY GTO ALGORITHM
In this paper, the GTO method is applied to obtain the optimal tap setting of the OLTC, the injected reactive power from the D-STATCOM, and the penetration of DGs-based RERs to satisfy the OF. It aims to minimize the total power losses, the number of Tap positions, and the total amount of curtailed PV and wind power. The proposed GTO method for solving the optimal coordination of voltage control problem is provided in the following section; flowchart and the architecture of the GTO method.

The first step in implementing the proposed coordination voltage control method is calculating the optimum locations of the DGs and the DSTATCOMs. Because this is out of the scope of this study, the optimum locations are obtained by executing the optimal power flow using the proposed GTO algorithm. After that, the optimal coordination of D-STATCOMs, OLTC transformers, and DG penetrations is obtained to control the voltage. The flowchart in Fig. 5 describes the flow steps of the proposed GTO algorithm. In this paper, each gorilla performs as a solution for the voltage coordination problem (the values of OLTC taps, size of D-STATCOMs, and size of the DGs). Also, the objective function acts as the fitness value of each gorilla.

The population, L_i, is initialized randomly and produced in the first step to determine the initial sets of the OLTC taps, the size of D-STATCOMs, and the size of the DGs. Also, the parameters of the GTO algorithm are selected as $\beta = 3$, $W = 0.8$, and $P = 0.03$ to direct the Gorilla Troops' movements in the search space. The proposed GTO in this study has six gorillas equal to the number of variables, and each gorilla represents a vector of ten elements. So, the Gorilla Troops is 6×10. Then the GTO algorithm will iterate to determine the optimal values of the OLTC taps, the size of D-STATCOMs, and the penetration of the DGs in the search space. In each iteration, the locations of the gorilla are modified by (26), (30), and (33) based on the K and C parameters.

The simulation is executed using MATLAB program with version R2019, a computer with operating system Windows 10, Intel Core i7 - 7500U CPU @ 2.7 GHz and 16.00 GB. All tests achieved to check the GTO performance are executed using 30 populations with maximum iterations of 200. The final results are saved based on the average of 25 independent run results.

VII. TEST SYSTEM
To evaluate the efficiency and capability of the proposed voltage method, two test systems are used under various conditions: NDEDC-24 bus radial distribution system and modified IEEE 33-node system.

A. NDEDC-24 BUS RADIAL DISTRIBUTION SYSTEM
A practical distribution system is considered under different conditions. The practical system is the NDEDC-24 bus radial distribution system from the NDEDC [56]. It is an 11 kV
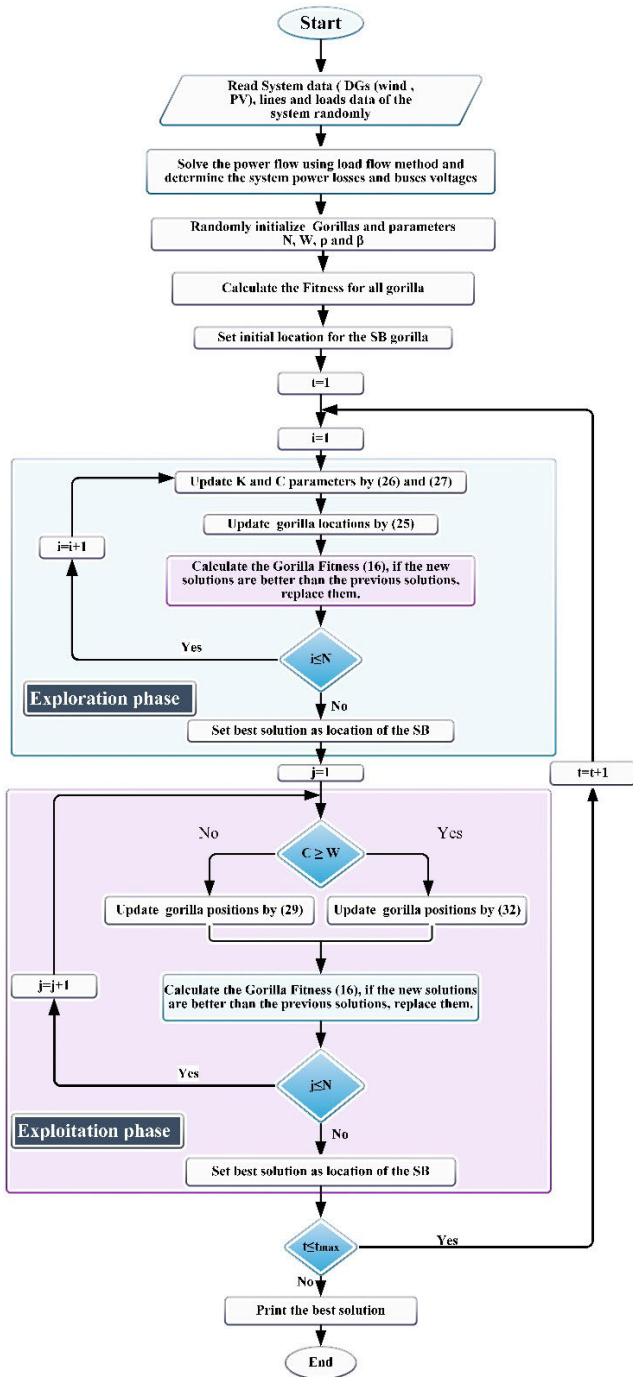
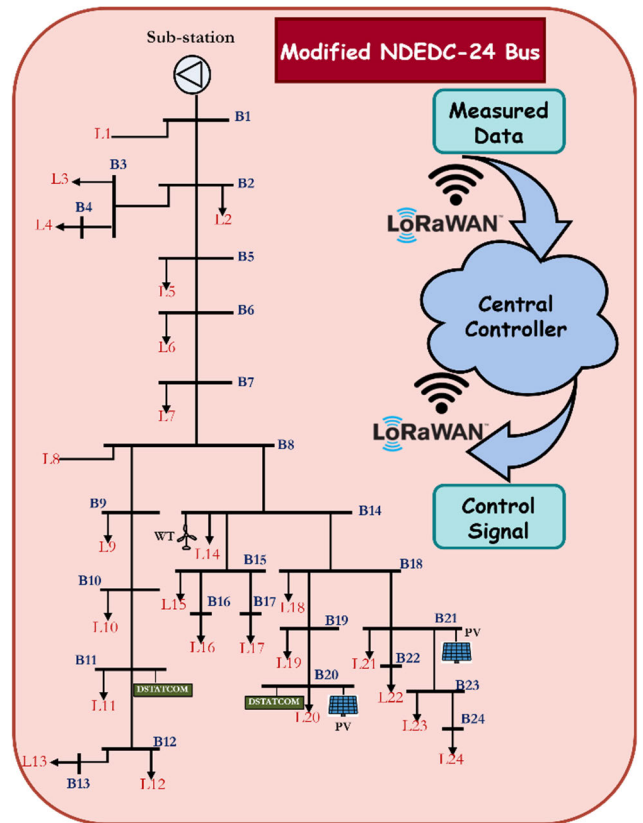**FIGURE 5.** Flowchart of the proposed GTO algorithm.

FIGURE 6. Modified single-line diagram of the NDEDC 24 bus test systems.

trated in Fig. 7, the peak load occurs from hours 18 to 20. Moreover, the data of the lines is included in the appendix.

Three DGs are installed at buses 14, 20, and 21 with maximum capacities of 750 kW, 1000 kVA, and 750 kW, respectively. This study applies two types of DGs-based renewable energy sources: PV panels and Wind turbines. The PV panels are located on buses 14 and 21, while the wind turbine is on buses 20. Figs. 8 and 9 illustrate the power generated from the DG sources (PV and Wind) for one day (24 hours). The D-STATCOM devices are installed on buses 11 and 20 with a maximum rating of 900 kVAR. The transformer under consideration is equipped with an OLTC mechanism on the primary winding installed at bus 14. The voltage range that can vary by the OLTC is equal to ±10% with a 2.5% step.

B. MODIFIED IEEE 33-NODE TEST SYSTEM
The modified IEEE 33-node system is selected as a standard system to verify the efficiency and accuracy of the proposed coordination method and test it. The single-line diagram and the parameters are given in previous work [39]. The output of the base load flow before installing DG, OLTC, and STATCOM with 100% loading is taken as the base case. In this test system, heavier operating conditions are imposed.

The total daily load curve is shown in Fig. 10. Three DGs are installed at buses 13, 15, and 31 with capacities of
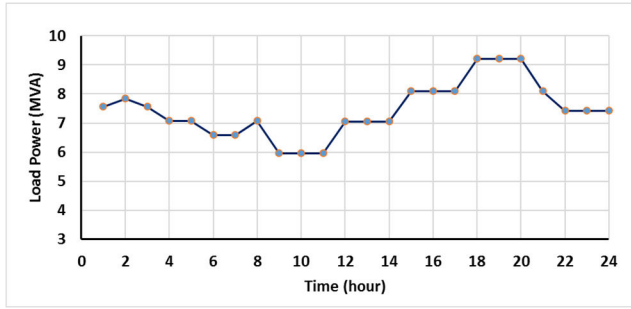
radial distribution network. The one-line diagram of the NDEDC-24 bus system is illustrated in Fig. 6. The maximum load of the test system is 10 MVA. Busbar B1 is the slack bus and has a constant voltage equal to 11kV ($1\angle 0°$).

The electric loads continuously fluctuate during the day. This is due to the different activities of the people. Furthermore, industrial and commercial power usage varies during the day. The total daily load curve is shown in Fig. 7. As illus-

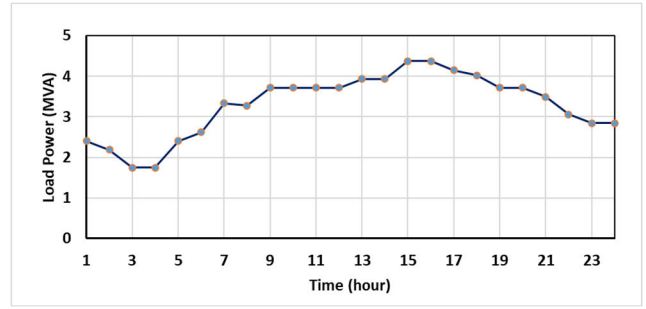**FIGURE 7.** Total daily load curve for the NDEDC-24 bus system.

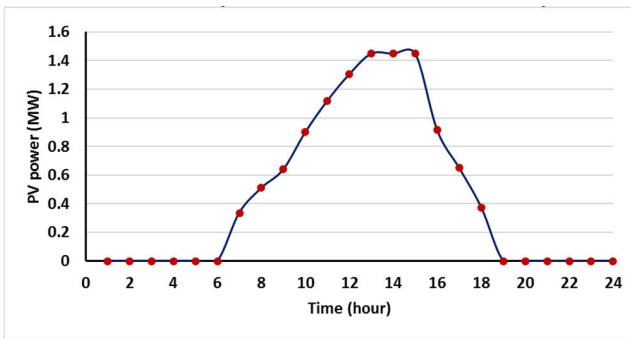**FIGURE 10.** Total daily load curve for IEEE 33-node system.

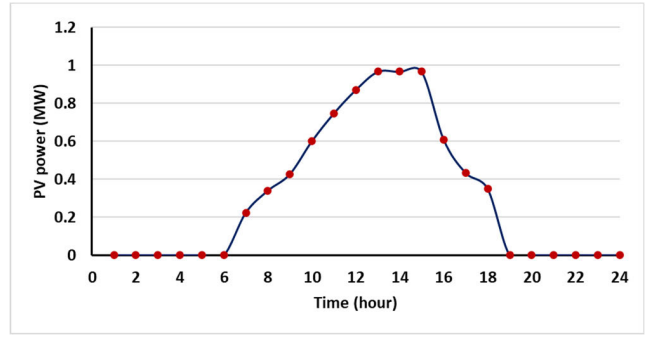**FIGURE 8.** Rated power generated from the PV panels during a day.

FIGURE 11. Rated power of PV panels for IEEE 33-node system during a day.
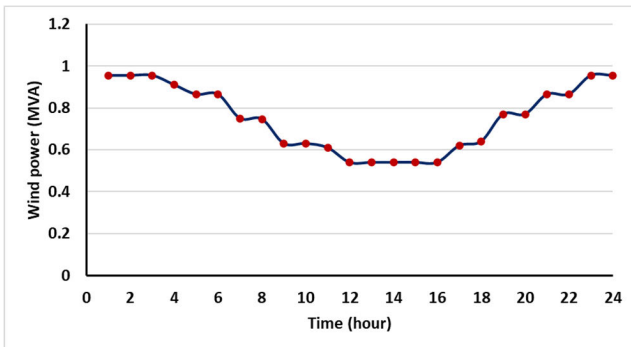

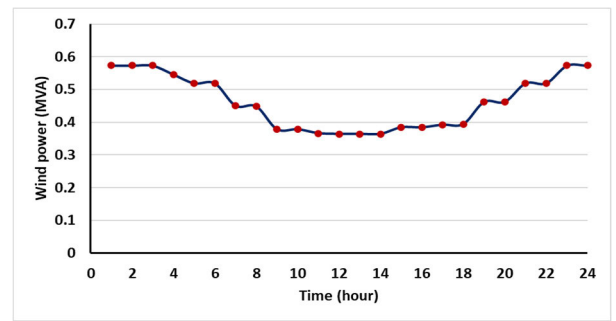**FIGURE 9.** Rated power generated from the wind turbine during a day.

FIGURE 12. Rated power generated from the wind turbine for IEEE 33-node system during a day.

500 kW, 500 kW, and 600 kVA, respectively. The PV panels are located at buses 13 and 15, while the wind turbine is on bus 31. Figures 11 and 12 illustrate the rated power produced from the PV and Wind sources for a day. Moreover, the STATCOM devices are installed on buses 19 and 25. Also, the OLTC is installed on bus 17.

VIII. RESULTS AND DISCUSSION

A. CASE STUDY 1: NDEDC-24 BUS TEST SYSTEM

Four different scenarios are applied to the NDEDC-24 bus test systems to evaluate the proposed voltage coordination method by combining different voltage control devices: DGs, D-STATCOMs, and OLTC. These scenarios are listed as follows:

Scenario 1: Without DGs and D-STATCOMs (base case)

Scenario 2: PV and D-STATCOMs
Scenario 3: Wind and D-STATCOMs
Scenario 4: PV, Wind, and D-STATCOMs

The results of these scenarios are illustrated in detail in the following subsections.

1) SCENARIO 1: WITHOUT DGs AND D-STATCOMs

In this scenario, the reactive power generation or consumption of the D-STATCOM and DGs is assumed to be zero. Peak demand on the 24-bus test system is 9.212 MVA in the base case, as shown in Fig. 7. The optimal load flow is performed on the test system during the day to determine the power losses in the feeders, voltage magnitudes at buses, and the tap settings of the OLTC. Figure 7 shows that the maximum load (9.212 MVA) and minimum (5.9616 MVA)
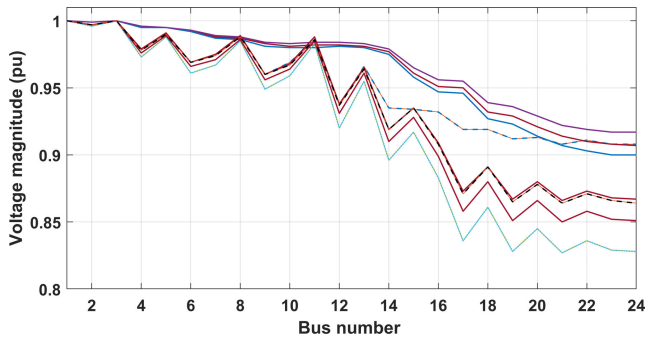
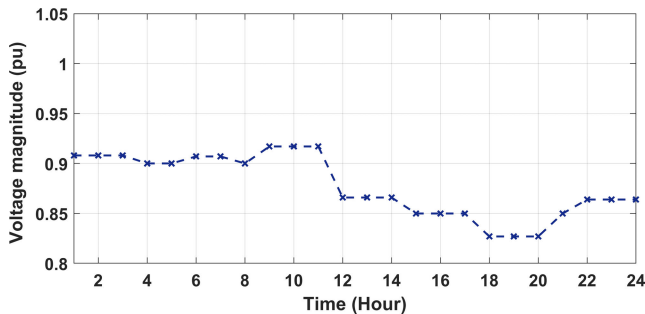**FIGURE 13.** Voltage profile without DGs and D-STATCOMs participation in voltage regulation.

FIGURE 14. Minimum voltage magnitude of the system without DGs and D-STATCOMs.

FIGURE 15. Total power losses of the system without DGs and D-STATCOMs.
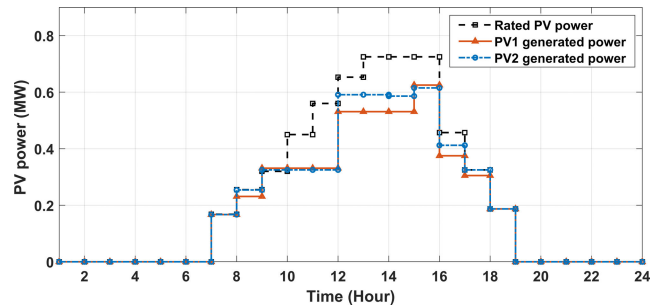
FIGURE 16. Generated power from the PV panels at buses 14 and 21 during a day.

occur at the 7th and 8th clocks, respectively. In this scenario, the voltage profile of each bus is illustrated in Fig. 13. Also, the minimum bus voltage magnitude during each hour of the day is illustrated in Fig. 14. From Figs. 13 and 14, it is found that the voltage profile performance is different for most buses. Also, during the day, the voltage varies, where the minimum voltage magnitude occurs at buses 19, 21, 23, and 24 with values less than 0.829 pu. This occurs during the day at hours 18, 19, and 20. In this base case, the D-STATCOMs and DGs are disconnected, and the voltage is less than the limit, 0.95 pu, at many buses, which is unacceptable for the DNs. In addition, the active and reactive power losses are obtained every hour during the day, as illustrated in Fig. 15. The main objectives of this paper are to keep the voltage within permissible limits and minimize power losses, waste energy of the DGs, and the number of TOs. So, the DGs, D-STATCOMs, and OLTC are used as control devices to satisfy these objectives.

2) SCENARIO 2: PVs AND D-STATCOMs

In this scenario, reducing the total number of TOs of the OLTC, minimizing the total active power losses, and the DG power curtailment is carried out for 11 kV 24-bus realistic time-varying DN with the integration of D-STATCOMs, DGs, and OLTC. Two PV panels are installed at buses 14 and 21 in the distribution network, while the D-STATCOM devices are connected to buses 11 and 20. Moreover, the OLTC is installed on bus 14. The optimal coordination of
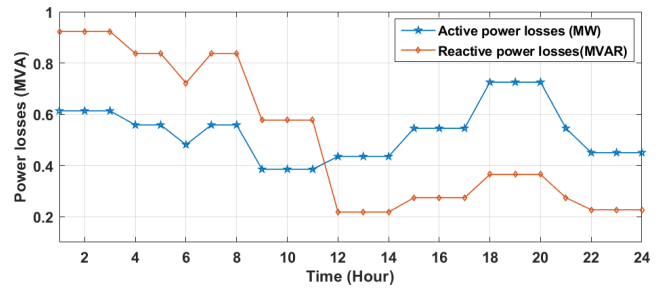
the OLTC, PV, and D-STATCOM is performed considering 24-hour PV and load variations. The optimal sizes of the PVs are determined using the proposed optimization algorithm based on the GTO to minimize the TP_L, PV panels, PC, and the TO of the OLTC while maintaining the voltage buses to their acceptable limitations.

The proposed GTO algorithm is applied to the test system in the presence of PVs, OLTC, and D-STATCOMs. The optimum active power generated from the PVs is shown in Fig. 16. Figure 17 illustrates the minimum voltage magnitude of the system during a day with and without connecting the D-STATCOMs and PV panels. It can be observed from Fig. 17 that, after switching the voltage control devices with the optimum setting values, the voltage profile is regulated within the acceptable limits throughout the test system. However, during the nighttime becomes slightly below the permissible set limits. It can also be observed from Figs. 16 and 17 that when the PV panels inject the highest power at 12:00 PM, the voltage magnitudes at the DG buses are near the upper limit. During the nighttime, the PV panels' output again becomes zero; however, the proposed coordination method effectively regulated the system buses' voltages magnitudes within acceptable limits by setting the optimum tap positions and the size of the D-STATCOMs.

The active and reactive power losses are illustrated in Fig. 18. The PVs and the D-STATCOMs can decrease the system's total reactive and active power losses compared to the base case. It is seen from Fig. 15 that the proposed coordination method can decrease the total active and reactive power losses in the test system lines from 12.717 to 6.941MW
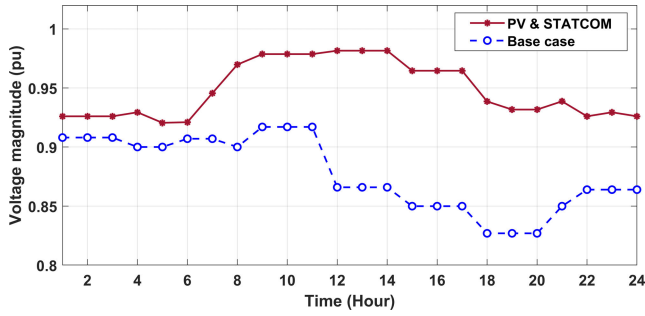
FIGURE 17. Minimum voltage magnitude of the system connected to the PV panel and D-STATCOMs.
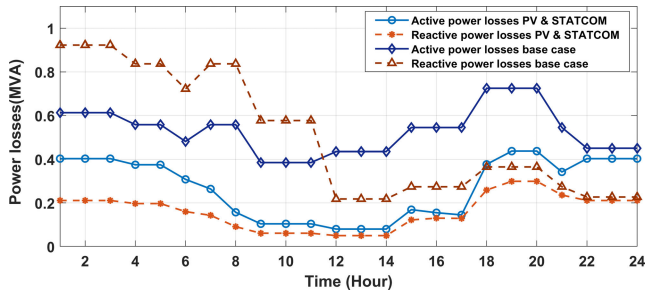

FIGURE 18. Power losses of the system connected to PV panels and D-STATCOMs.

FIGURE 19. Generated power from the wind turbines at bus 20.

FIGURE 20. Minimum voltage magnitude of the system connected to wind turbine and D-STATCOMs.

FIGURE 21. Power losses of the system connected to the wind turbine and D-STATCOMs.

and from 12.096 to 5.861 MVAR compared to the base case for one day, respectively.

By using the OLTC action only to regulate the voltage for the test system, as in the base case, there is multiple switching of the TOs to maintain the voltage. The number of TOs of the OLTC is minimized with coordination between OLTC and D-STATCOMs and optimal integration of DG-based PV panels, which is reduced from 16 to 13 operations during a day (24 hours), and the voltage profile is kept within permissible limits.

3) SCENARIO 3: WIND AND D-STATCOMs
A wind power DG-based DFIG rating of 1000 kVA is connected to bus 20 in the test system. The proposed GTO algorithm is implemented in the test system to determine the optimal values of the power generated from the wind turbine, the settings of the taps of the OLTC, and the ratings of the D-STATCOMs during the day. These values are obtained to minimize the TPL, wind turbine PC, and TOs while maintaining the voltage buses to their acceptable limitations.

Figure 19 illustrates the optimal values of wind turbine-generated power at bus 20 for a 24-hour time-varying load model. It can be seen from Fig. 19 that the generated wind power is affected by the rated power curve and the load changes. The wind turbine PC is demonstrated by the difference between the rated wind turbine power and the actual generated power, as shown in Fig. 19. The voltage profile improvement is depicted in Fig. 20, where the minimum voltage magnitude is improved from 0.826 pu (base case) to 0.9228 pu at bus 18. It is also worth noting that the maximum
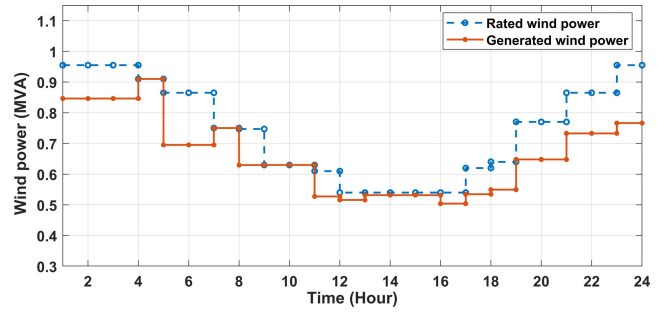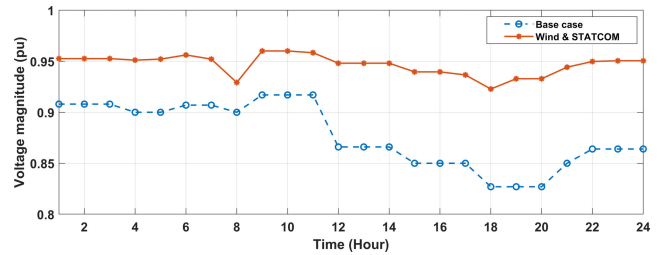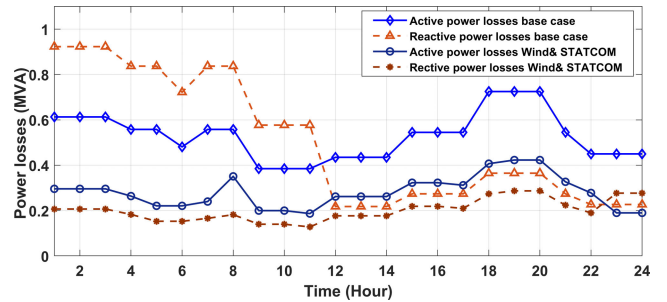
value of the voltage magnitude is 1.0078 pu at bus 14 due to the OLTC effect.

By applying the proposed GTO algorithm, the values of the system's total active and reactive power losses during a day (24 hours) are reduced, as illustrated in Fig. 21. It decreased to 6.554 MW from 12.717 MW (24 hours) without connecting wind turbines and D-STATCOMs. Moreover, the power losses, in this case, are lower than those for connected PV panels and D-STATCOMs (6.941 MW). This is due to the continuous generation of power from wind turbines, unlike PV panels that only generate power during the day. Also, the total number of TOs of the OLTC is reduced to 10 switching operations during a day (24 hours) which is lower than scenarios 1 and 2, and the voltage profile is kept within permissible limits.

4) SCENARIO 4: PVs, WIND, AND D-STATCOMs
As in the previous scenario, a DFIG-based wind power DG rating of 955 kVA is connected to bus 20. Also, two PV panels are installed at buses 14 and 21, and the D-STATCOM devices are installed at buses 11 and 20 in the tested DN. Moreover, the OLTC transformer is connected to bus 14.
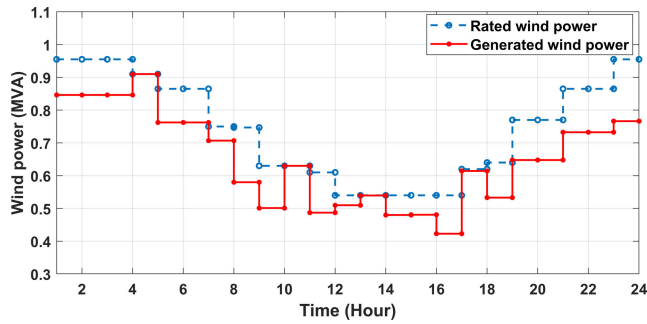
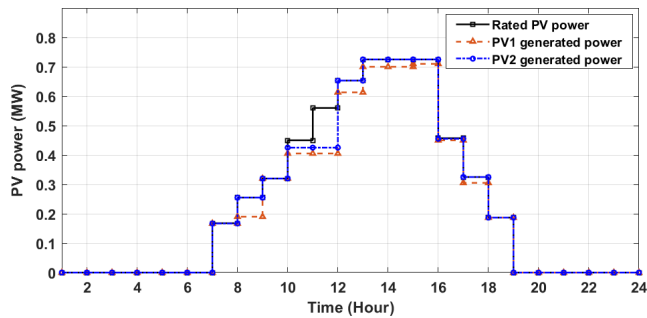**FIGURE 22.** Generated power from the wind turbines at bus 20.

FIGURE 23. Generated power from the PV panels at buses 14 and 21.
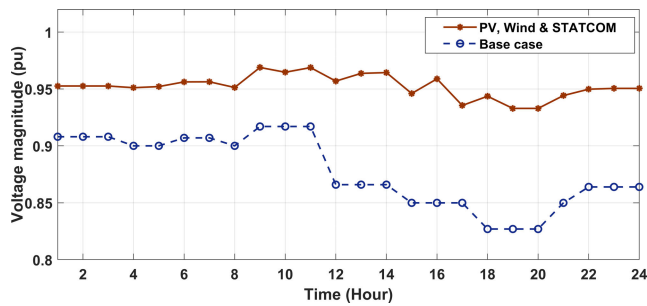

FIGURE 24. Minimum voltage magnitude of the system connected to PV panel, wind turbine, and D-STATCOMs.
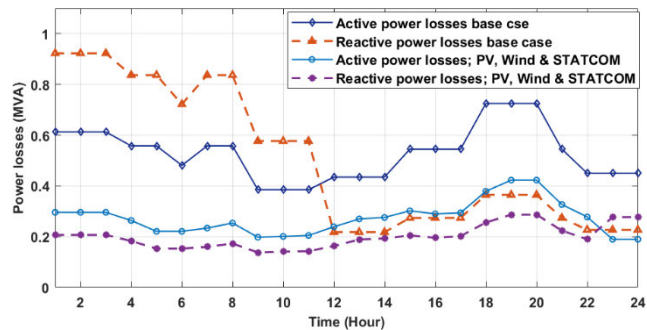

FIGURE 25. Power losses of the system connected to the PV panel, wind turbine, and D-STATCOMs.

The optimal coordination of the OLTC, PVs, wind turbine, and D-STATCOMs is performed considering 24-hour with PVs and wind power generation and load variations. The optimal sizes of the PVs, wind turbine, and D-STATCOMs are calculated using the proposed optimization algorithm based on the GTO to minimize the TP_L, DG generation (PV panels and wind turbine), PC, and the TO of the OLTC while
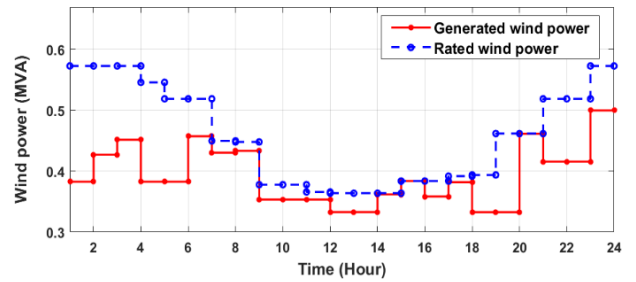

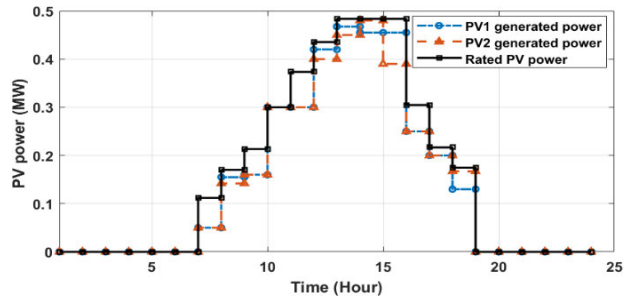**FIGURE 26.** Generated power from the wind turbines at bus 31.

FIGURE 27. Generated power from the PV panels at buses 13 and 15.

maintaining the voltage buses to their acceptable limitations. It is interesting to note that this case is unlike other test cases. This scenario is divided into two stages. In the first stage, two PV panels from 1:6 PM and 19:23 AM are not considered, but a doubly fed induction generator-based wind power DG is working all day. Second stage, from 6:00 PM to 19:00 AM, two PV panels, DFIG, D-STATCOMs, and OLTC, are working in series. The optimal power values generated from the two PV panels and wind turbines are calculated using the proposed GTO algorithm. Settings of the taps of the OLTC and the ratings of the D-STATCOMs during the day are also determined. These values are obtained to minimize the TPL, wind generation PC, and TOs while maintaining the voltage buses to their acceptable limitations compared with the previous cases. The values of the system's total active and reactive power losses during the day (24 hours) are reduced. It decreased to 5.467 MW from 12.717 MW (24 hours) without connecting DGs and D-STATCOMs. Moreover, the power losses, in this case, are lower than those for connected PV panels and D-STATCOMs (6.554 MW). This is due to the continuous generation of power from wind turbines, unlike PV panels that only generate power during the day.

Figures 22 and 23 show the change in active and reactive powers of the DFIG and PVs. The minimum voltage magnitudes during 24 hours for this scenario and the base scenario are illustrated in Fig. 24. At 8:00 PM, the system voltages start to rise due to an increase in the PV panels generated power. At 19:00 PM, the voltage starts to decrease because the PVs outputs declined. The new tap position and active power set points were calculated and changed again due to the violation of the voltage set limit. Figure 25 illustrates the active and reactive power losses for this scenario. It proves that the proposed method can reduce the power losses in this scenario more than the other scenarios. The results presented
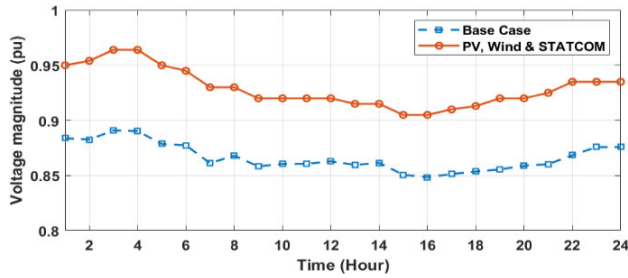
FIGURE 28. Minimum voltage magnitude of the system connected to PV panel, wind turbine, and D-STATCOMs.
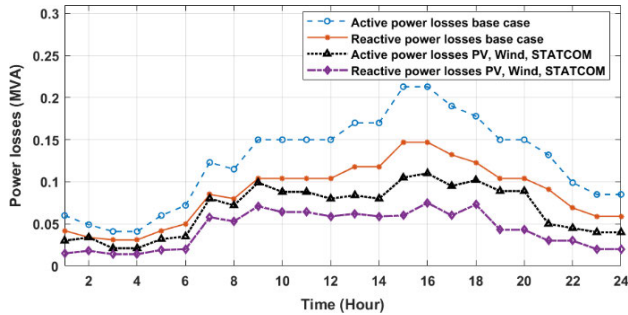

FIGURE 29. Power losses of the system connected to the PV panel, wind turbine, and D-STATCOMs.

in Figures 22 to 25 demonstrate that the proposed coordination method not only optimizes the reactive and active power of losses of the DNs, but also controls the power of DGs and the acceptable limits of the buses' voltages. Also, the total number of TOs of the OLTC is reduced to 8 switching operations during a day (24 hours) which is the lowest one in the previous scenarios.

B. CASE STUDY 2: MODIFIED IEEE 33-NODE TEST SYSTEM

The proposed coordination method is implemented on a standard distribution system: a modified IEEE 33-node test system. The proposed method based on GTO is used to calculate the optimal generated power from DG sources (PV panels and Wind), the size of the DSTATCOM, and the setting of the OLTC to minimize the TP_L DG sources the PC and the TO of the OLTC while maintaining the voltage buses to their acceptable limitations.

Applying the proposed method decreases the power losses to 2.059 MW from 2.996 MW (24 hours) without connecting the DGs and the D-STATCOMs. Figures 26 and 27 show the change in active and reactive powers of the DFIG and PVs. The minimum voltage magnitudes during 24 hours for this scenario and the base scenario are illustrated in Fig. 28. Figure 29 illustrates the active and reactive power losses for this scenario. It proves that the proposed method can reduce power losses.

The results presented in Figures 26 to 29 demonstrate that the proposed coordination method optimizes the reactive and active power of losses of the DNs and controls the power of DGs and the acceptable limits of the buses' voltages. Also, the total number of TOs of the OLTC is reduced to 4 switching operations during a day (24 hours).
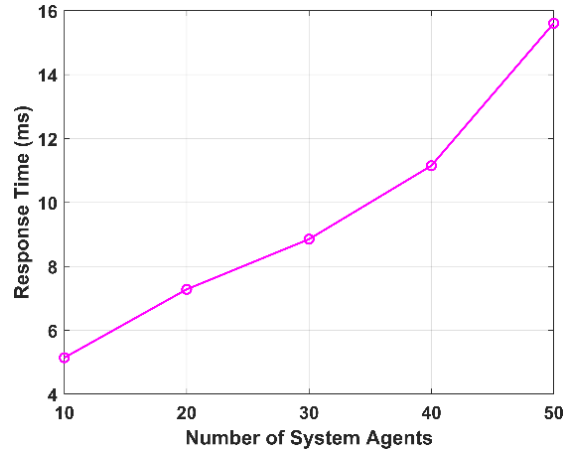
FIGURE 30. Time response for the proposed IoT platform.
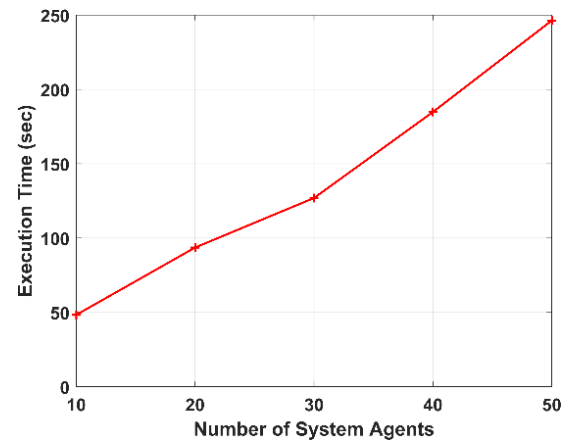
FIGURE 31. Execution time for the proposed IoT platform.
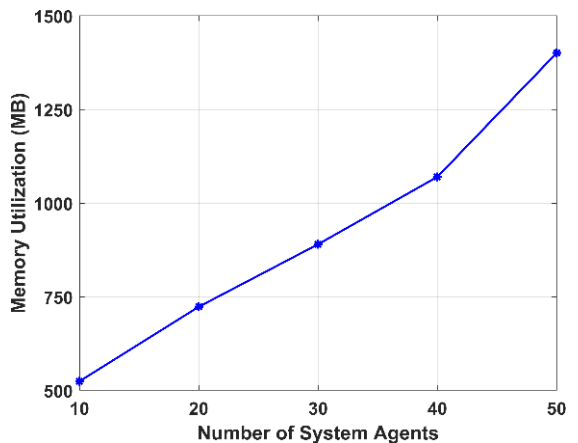
FIGURE 32. Memory used for the proposed IoT platform.

C. PERFORMANCE EVALUATION OF THE PROPOSED IoT PLATFORM

The IoT platform has been proposed and applied to communicate with all the system agents and monitor all the required data and information in the SDN. To evaluate the performance of the proposed communication channel, the time response, execution time, and the memory size required is extracted. The response time is the time required to respond to any

FIGURE 33. Variation of the objective function with the iteration number.

TABLE 1. Comparison between the various applied scenarios.

Scenarios	Base Case	PV & D-STATCOMs	Wind & D-STATCOMs	PV, Wind & D-STATCOMs
Minimum voltage magnitude	0.827	0.9205	0.9228	0.9329
Maximum voltage magnitude	1	1.0251	1.0078	1.0176
Total active power losses	12.717	6.941	6.554	5.467
Total reactive power losses	12.096	5.861	4.861	4.811
Total number of OTs	16	13	10	8

TABLE 2. Comparison with other existing optimization techniques.

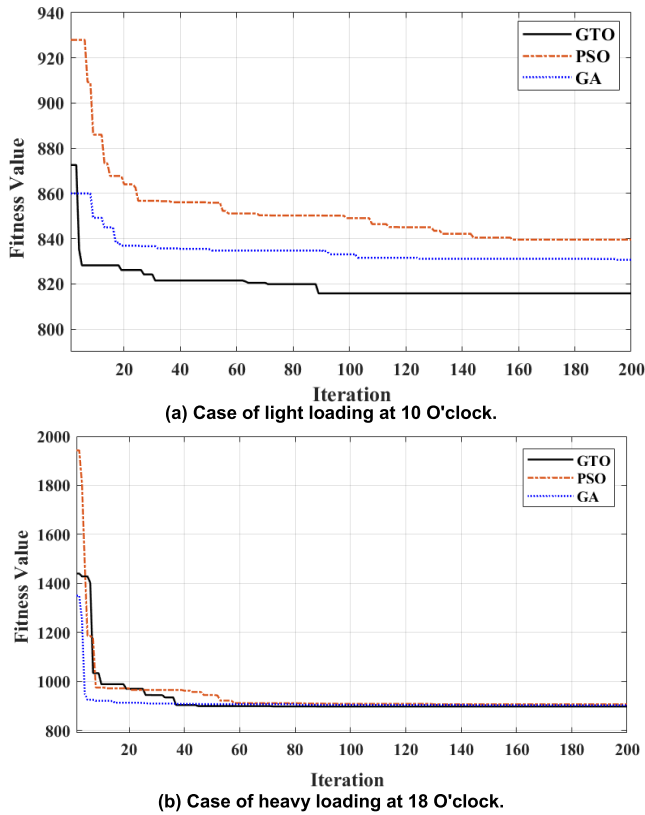| Scenarios	Base Case	multi-objective PSO	GA	Proposed method-based GTO
Minimum voltage magnitude	0.827	0.9213	0.9156	0.9329
Maximum voltage magnitude	1	1.008	1.004	1.0176
Total active power losses	12.717	8.277	8.0153	5.467
Total reactive power losses	12.096	7.431	7.123	4.811
Total number of OTs	16	10	10	8

change in the SDN. The execution time is the required time for the whole system to make a control decision. It includes measuring data, communication, processing, and controlling signal time. The system agents include the DGs, OLTCs, and D-STATCOMs data. With increasing the system agents, the execution time is increased. Hence, the memory size required for data storage is increased. Also, the response time for the proposed method is increased. The LoRaWAN communication channel has 868 MHz [67], with a 1.15 ms delay time. Figure 30 shows the proposed IoT platform response time with changing the system agent's number. The execution time has been evaluated according to the changing of the system agents, as shown in Fig. 31. While Fig. 32 illustrates the relation between the number of the system's agents and the memory size. The results show that the proposed IoT platform can respond, execute, and process the data in a reasonable time.

D. COMPARATIVE ANALYSIS

In general, the proposed method for optimal coordination of voltage control devices can keep the buses' voltage magnitudes at the permissible limits while minimizing the power losses of the feeders, waste energy of the DGs-based RERs, and the number of tap operations of the OLTCs. The fourth scenario is most effective and more efficient than the other scenarios due to the nature of the energy generation of the RERs. Wind turbines and PV panels have opposite performances for the power generation curve throughout the day. Table 1 summarizes a comparison between the different scenarios. It illustrates that scenario four is more effective in

reducing the power losses, energy wastage from DGs, and the number of TOs of OLTC. So, this scenario can effectively decrease the operating cost of SDNs.

The proposed method for optimal coordination of voltage control devices-based GTO performance is compared with the previous methods using the same distribution feeder and operating conditions in scenario four. The multi-objective PSO [39] and GA [37] are applied to the NDEDC-24 bus radial distribution system from the NDEDC, as illustrated in Fig. 6. Table 2 illustrates the results and the performances of these optimization methods. It can be seen that the proposed method for optimal coordination of voltage control devices-based GTO outperformed the previous methods. Figure 33 illustrates the convergence curves of the three optimization algorithms, GTO, PSO, and GA, for two selected cases of system loading. The first case is at 10 o'clock when the load is minimum, and the second is at the maximum load at 18 o'clock. The fitness values are determined when connecting the PV panel, wind turbine, and D-STATCOMs to the NDEDC-24 bus radial distribution system. The Figures show that the GTO converges faster than PSO and GA. Also, it produces the best solution, which results in minimum power losses and DGs' energy wastage and the number of OLTC-tap operations.

IX. CONCLUSION

This paper presented a centralized voltage coordination method for the D-STATCOMs, OLTC, and DGs in the SDNs. This method is based on the GTO algorithm to calculate the best voltage coordination solution. SDN architecture was designed using IoT technology for data and information transfer capabilities. Four layers were implemented for the SDN-based physical, communication, processing, and cyber layers. LoRaWAN communication channel was applied for data transfer between agents and central controllers. The following findings were obtained.

1- The proposed coordination method could minimize the power losses, DGs' energy wastage, and the number of OLTC-tap operations while maintaining the voltages at acceptable limits in all scenarios.

2- Several scenarios with different DG types were applied to test the efficacy of the proposed control system: combined PVs, OLTC, and D-STATCOMs, combined wind turbine, OLTC, and D-STATCOMs, and combined the PVs, wind turbines, OLTC, and D-STATCOMs.

3- Scenario 3 of PV, Wind, and D-STATCOM was more effective than the other scenarios.
  - The active power losses were reduced by 57.01%.
  - The reactive power losses were reduced by 60.22%
  - The total number of OTs of the OLTC was reduced by 50%.
  - The minimum and maximum bus voltage values during the day were within the acceptable limits of 0.9329 and 1.0176 pu, respectively.

4- A new optimization method based on the GTO was used in this paper to find the optimum settings of the D-STATACOMs, DGs, and OLTCs.

5- The proposed GTO algorithm showed high accuracy in obtaining the optimal settings of the D-STATACOMs, DGs, and OLTCs.

6- The proposed GTO was compared with PSO and GA. The comparative evaluation showed that the proposed GTO enjoyed the highest accuracy and required lowest computation time.

7- The Weibull PDF was used to model the uncertainty of natural wind speed and solar irradiance.

8- Generally, the results led to enhancing the utilization of the power generated from the RERs (PV and wind) and reducing energy waste. It also reduced the power losses and the number of tap operations of the OLTC; thus, it reduced the operating costs of the SDNs.

APPENDIX

See Tables 3 and 4.

ACKNOWLEDGMENT

TABLE 3. A1 NDEDC 24-bus system lines data.

Line No.	Sending End bus	Receiving End bus	R (Ω)	X (Ω)	Maximum Line Capacity (A)
1	1	2	0.6762	1.235	585
2	2	3	0.2646	0.423	140
3	3	4	0.3542	0.319	140
4	2	5	0.3864	0.1739	585
5	5	6	0.3864	0.346	585
6	6	7	0.117	0.214	585
7	7	8	0.056	0.11	585
8	9	9	0.029	0.023	140
9	9	10	0.773	0.696	140
10	10	11	0.837	0.402	140
11	11	12	0.386	0.185	140
12	12	13	0.0882	0.161	140
13	8	14	0.257	0.232	300
14	14	15	0.132	0.242	140
15	15	16	0.552	0.497	140
16	15	17	0.264	0.484	140
17	14	18	0.46	0.22	300
18	18	19	0.0129	0.116	140
19	19	20	0.193	0.174	140
20	18	21	0.332	0.29	140
21	21	22	0.332	0.29	140
22	21	23	0.0193	0.182	140
23	23	24	0.0257	0.243	140

TABLE 4. A2 NDEDC 24-bus system distribution transformers data.

Transformer No.	Rating	Transformer No.	Rating
1	1000	13	500
2	100	14	160
3	1000	15	200
4	500	16	200
5	160	17	160
6	200	18	800
7	800	19	500
8	500	20	200
9	100	21	500
10	300	22	300
11	300	23	300
12	300	24	200

REFERENCES

[1] P. Chaudhary and M. Rizwan, "Voltage regulation mitigation techniques in distribution system with high PV penetration: A review," *Renew. Sustain. Energy Rev.*, vol. 82, pp. 3279–3287, Feb. 2018.

[2] E. Hamza, B. Sedhom, and E. Badran, "Impact and assessment of the overvoltage mitigation methods in low-voltage distribution networks with excessive penetration of PV systems: A review," *Int. Trans. Electr. Energy Syst.*, vol. 31, no. 12, 2021, Art. no. e13161.

[3] A. M. M. Nour, A. Y. Hata, A. A. Helal, and M. M. El-Saadawi, "Review on voltage-violation mitigation techniques of distribution networks with distributed rooftop PV systems," *IET Gener., Transmiss. Distrib.*, vol. 14, no. 3, pp. 349–361, Feb. 2020.

[4] A. Iqbal, A. Waqar, R. M. Elavarasan, M. Premkumar, T. Ahmed, U. Subramaniam, and S. Mekhilef, "Stability assessment and performance analysis of new controller for power quality conditioning in microgrids," *Int. Trans. Electr. Energy Syst.*, vol. 31, no. 6, Jun. 2021, Art. no. e12891.

[5] S. B. Pandu, C. K. Sundarabalan, N. S. Srinath, T. S. Krishnan, G. S. Priya, C. Balasundar, J. Sharma, G. Soundarya, P. Siano, and H. H. Alhelou, "Power quality enhancement in sensitive local distribution grid using interval type-II fuzzy logic controlled DSTATCOM," *IEEE Access*, vol. 9, pp. 59888–59899, 2021.

[6] R. Kumar, S. Diwania, P. Khetrapal, S. Singh, and M. Badoni, "Multimachine stability enhancement with hybrid PSO-BFOA based PV-STATCOM," *Sustain. Comput., Informat. Syst.*, vol. 32, Dec. 2021, Art. no. 100615.

[7] C. M. Castiblanco-Pérez, D. E. Toro-Rodríguez, O. D. Montoya, and D. A. Giral-Ramírez, "Optimal placement and sizing of D-STATCOM in radial and meshed distribution networks using a discrete-continuous version of the genetic algorithm," *Electronics*, vol. 10, no. 12, p. 1452, Jun. 2021.

[8] A. S. Siddiqui, M. Sarwar, A. Althobaiti, and S. S. M. Ghoneim, "Optimal location and sizing of distributed generators in power system network with power quality enhancement using fuzzy logic controlled D-STATCOM," *Sustainability*, vol. 14, no. 6, p. 3305, Mar. 2022.

[9] O. D. Montoya, A. Garces, and W. Gil-González, "Minimization of the distribution operating costs with D-STATCOMS: A mixed-integer conic model," *Electric Power Syst. Res.*, vol. 212, Nov. 2022, Art. no. 108346.

[10] O. D. Montoya, A. Molina-Cabrera, D. A. Giral-Ramírez, E. Rivas-Trujillo, and J. A. Alarcón-Villamil, "Optimal integration of D-STATCOM in distribution grids for annual operating costs reduction via the discrete version sine-cosine algorithm," *Results Eng.*, vol. 16, Dec. 2022, Art. no. 100768.

[11] J. Sanam, "Optimization of planning cost of radial distribution networks at different loads with the optimal placement of distribution STATCOM using differential evolution algorithm," *Soft Comput.*, vol. 24, no. 17, pp. 13269–13284, Sep. 2020.

[12] J. Sanam, A. K. Panda, and S. Ganguly, "Optimal phase angle injection for reactive power compensation of distribution systems with the allocation of multiple distribution STATCOM," *Arabian J. Sci. Eng.*, vol. 42, no. 7, pp. 2663–2671, Jul. 2017.

[13] A. Kavousi-Fard and M.-R. Akbari-Zadeh, "Probabilistic multiple distribution static compensator placement and sizing based on the two-point estimate method," *Int. J. Sustain. Energy*, vol. 33, no. 6, pp. 1041–1053, Nov. 2014.

[14] A. S. Saidi, "Impact of grid-tied photovoltaic systems on voltage stability of Tunisian distribution networks using dynamic reactive power control," *Ain Shams Eng. J.*, vol. 13, no. 2, Mar. 2022, Art. no. 101537.

[15] R. Anilkumar, G. Devriese, and A. K. Srivastava, "Voltage and reactive power control to maximize the energy savings in power distribution system with wind energy," *IEEE Trans. Ind. Appl.*, vol. 54, no. 1, pp. 656–664, Jan. 2018.

[16] E. O. Hasan, A. Y. Hatata, E. A.-E. Badran, and F. H. Yossef, "Voltage control of distribution systems using electronic OLTC," in *Proc. 20th Int. Middle East Power Syst. Conf. (MEPCON)*, Dec. 2018, pp. 18–20.

[17] E. O. Hasan, A. Y. Hatata, E. A. Badran, and F. M. H. Yossef, "A new strategy based on ANN for controlling the electronic on-load tap changer," *Int. Trans. Electr. Energy Syst.*, vol. 29, no. 10, p. e1206, Oct. 2019.

[18] M. M. Rahman, A. Arefi, G. M. Shafiullah, and S. Hettiwatte, "A new approach to voltage management in unbalanced low voltage networks using demand response and OLTC considering consumer preference," *Int. J. Electr. Power Energy Syst.*, vol. 99, pp. 11–27, Jul. 2018.

[19] M. A. Shaik, P. L. Mareddy, and N. Visali, "Enhancement of voltage profile in the distribution system by reconfiguring with DG placement using equilibrium optimizer," *Alexandria Eng. J.*, vol. 61, no. 5, pp. 4081–4093, May 2022.

[20] M. T. Rahman, K. N. Hasan, and P. Sokolowski, "Assessment of conservation voltage reduction capabilities using load modelling in renewable-rich power systems," *IEEE Trans. Power Syst.*, vol. 36, no. 4, pp. 3751–3761, Jul. 2021.

[21] P. Paliwal, "Comprehensive analysis of distributed energy resource penetration and placement using probabilistic framework," *IET Renew. Power Gener.*, vol. 15, no. 4, pp. 794–808, Mar. 2021.

[22] A. S. A. Awad, D. Turcotte, and T. H. M. El-Fouly, "Impact assessment and mitigation techniques for high penetration levels of renewable energy sources in distribution networks: Voltage-control perspective," *J. Modern Power Syst. Clean Energy*, vol. 10, no. 2, pp. 450–458, 2022.

[23] S. Oliva H., J. Muñoz, F. Fredes, and E. Sauma, "Impact of increasing transmission capacity for a massive integration of renewable energy on the energy and environmental value of distributed generation," *Renew. Energy*, vol. 183, pp. 524–534, Jan. 2022.

[24] M. Saric, J. Hivziefendic, T. Konjic, and A. Ktena, "Distributed generation allocation considering uncertainties," *Int. Trans. Electr. Energy Syst.*, vol. 28, no. 9, p. e2585, Sep. 2018.

[25] L. D. L. Pereira, I. Yahyaoui, R. Fiorotti, L. S. De Menezes, J. F. Fardin, H. R. O. Rocha, and F. Tadeo, "Optimal allocation of distributed generation and capacitor banks using probabilistic generation models with correlations," *Appl. Energy*, vol. 307, Feb. 2022, Art. no. 118097.

[26] N. Mansouri, A. Lashab, J. Guerrero, and A. Cherif, "Photovoltaic power plants in electrical distribution networks: A review on their impact and solutions," *IET Renew. Power Gener.*, vol. 14, no. 12, pp. 2114–2125, 2020.

[27] J. Martins, S. Spataru, D. Sera, D.-I. Stroe, and A. Lashab, "Comparative study of ramp-rate control algorithms for PV with energy storage systems," *Energies*, vol. 12, no. 7, p. 1342, Apr. 2019.

[28] N. Mansouri, A. Lashab, D. Sera, J. M. Guerrero, and A. Cherif, "Large photovoltaic power plants integration: A review of challenges and solutions," *Energies*, vol. 12, no. 19, p. 3798, Oct. 2019.

[29] A. Selim, S. Kamel, A. A. Mohamed, and E. E. Elattar, "Optimal allocation of multiple types of distributed generations in radial distribution systems using a hybrid technique," *Sustainability*, vol. 13, no. 12, p. 6644, Jun. 2021.

[30] M. H. Ali, S. Kamel, M. H. Hassan, M. Tostado-Véliz, and H. M. Zawbaa, "An improved wild horse optimization algorithm for reliability based optimal DG planning of radial distribution networks," *Energy Rep.*, vol. 8, pp. 582–604, Nov. 2022.

[31] M. S. Alanazi, "A MILP model for optimal renewable wind DG allocation in smart distribution systems considering voltage stability and line loss," *Alexandria Eng. J.*, vol. 61, no. 8, pp. 5887–5901, Aug. 2022.

[32] R. Sellami, F. Sher, and R. Neji, "An improved MOPSO algorithm for optimal sizing & placement of distributed generation: A case study of the Tunisian offshore distribution network (ASHTART)," *Energy Rep.*, vol. 8, pp. 6960–6975, Nov. 2022.

[33] Y. J. Kim, J. L. Kirtley, and L. K. Norford, "Reactive power ancillary service of synchronous DGs in coordination with voltage control devices," *IEEE Trans. Smart Grid*, vol. 8, no. 2, pp. 515–527, Sep. 2015.

[34] K. K. Mehmood, S. U. Khan, S.-J. Lee, Z. M. Haider, M. K. Rafique, and C.-H. Kim, "A real-time optimal coordination scheme for the voltage regulation of a distribution network including an OLTC, capacitor banks, and multiple distributed energy resources," *Int. J. Electr. Power Energy Syst.*, vol. 94, pp. 1–14, Jan. 2018.

[35] M. Chamana and B. H. Chowdhury, "Optimal voltage regulation of distribution networks with cascaded voltage regulators in the presence of high PV penetration," *IEEE Trans. Sustain. Energy*, vol. 9, no. 3, pp. 1427–1436, Jul. 2018.

[36] L. Jiaming, H. Qunhai, Y. Jingyuan, L. Qiran, S. Longfei, and W. Tongzhen, "Study on coordinated voltage regulation strategy of flexible on-load tap changer and distributed generator," in *Proc. 5th Int. Conf. Electr. Eng. Green Energy, (CEEGE)*, Berlin, Germany, Nov. 2022, pp. 601–609.

[37] M. Aryanezhad, "Management and coordination of LTC, SVR, shunt capacitor and energy storage with high PV penetration in power distribution system for voltage regulation and power loss minimization," *Int. J. Elect. Power Energy Syst.*, vol. 100, pp. 178–192, Sep. 2018.

[38] Y. Xu, Z. Y. Dong, R. Zhang, and D. J. Hill, "Multi-timescale coordinated voltage/var control of high renewable-penetrated distribution systems," *IEEE Trans. Power Syst.*, vol. 32, no. 6, pp. 4398–4408, Nov. 2017.

[39] E. O. Hasan, A. Y. Hatata, E. A. Badran, and F. M. H. Yossef, "Optimal coordination of voltage control devices in distribution systems connected to distributed generations," *Electr. Eng.*, vol. 101, no. 1, pp. 175–187, Apr. 2019.

[40] A. Nasef, A. Shaheen, and H. Khattab, "Local and remote control of automatic voltage regulators in distribution networks with different variations and uncertainties: Practical cases study," *Electric Power Syst. Res.*, vol. 205, Apr. 2022, Art. no. 107773.

[41] T. Samakpong, W. Ongsakul, and N. M. Manjiparambil, "Optimal power flow incorporating renewable uncertainty related opportunity costs," *Comput. Intell.*, vol. 38, no. 3, pp. 1057–1082, Jun. 2022.

[42] A. Ramadan, M. Salah, K. Emad, M. Marcos, and T. Veliz, "Optimal allocation of renewable DGs using artificial hummingbird algorithm under uncertainty conditions," *Ain Shams Eng. J.*, vol. 14, no. 2, 2022, Art. no. 101872.

[43] M. Hemeida, S. Alkhalaf, T. Senjyu, A. Ibrahim, M. Ahmed, and A. Bahaa-Eldin, "Optimal probabilistic location of DGs using Monte Carlo simulation based different bio-inspired algorithms," *Ain Shams Eng. J.*, vol. 12, no. 3, pp. 2735–2762, 2021.

[44] S. Lv, J. Li, Y. Guo, and Z. Shi, "A typical distributed generation scenario reduction method based on an improved clustering algorithm," *Appl. Sci.*, vol. 9, no. 20, p. 4262, Oct. 2019.

[45] F. S. Al-Ismail, "DC microgrid planning, operation, and control: A comprehensive review," *IEEE Access*, vol. 9, pp. 36154–36172, 2021.

A. Y. Hatata et al.: Centralized Control Method for Voltage Coordination Challenges With OLTC and D-STATCOM

[46] D. Espín-Sarzosa, R. Palma-Behnke, and O. Nuñez-Mata, "Energy management systems for microgrids: Main existing trends in centralized control architectures," *Energies*, vol. 13, no. 3, p. 547, Jan. 2020.

[47] M. Mehdi, C.-H. Kim, and M. Saad, "Robust centralized control for DC islanded microgrid considering communication network delay," *IEEE Access*, vol. 8, pp. 77765–77778, 2020.

[48] J. M. Raya-Armenta, N. Bazmohammadi, J. G. Avina-Cervantes, D. Sáez, J. C. Vasquez, and J. M. Guerrero, "Energy management system optimization in islanded microgrids: An overview and future trends," *Renew. Sustain. Energy Rev.*, vol. 149, Oct. 2021, Art. no. 111327.

[49] T. Ahmad and D. Zhang, "Using the Internet of Things in smart energy systems and networks," *Sustain. Cities Soc.*, vol. 68, May 2021, Art. no. 102783.

[50] A. H. Siddique, S. Tasnim, F. Shahriyar, M. Hasan, and K. Rashid, "Renewable energy sector in Bangladesh: The current scenario, challenges and the role of IoT in building a smart distribution grid," *Energies*, vol. 14, no. 16, p. 5083, Aug. 2021.

[51] M. S. Hossain, M. Rahman, M. T. Sarker, M. E. Haque, and A. Jahid, "A smart IoT based system for monitoring and controlling the sub-station equipment," *Internet Things*, vol. 7, Sep. 2019, Art. no. 100085.

[52] A. A. A. Sen and M. Yamin, "Advantages of using fog in IoT applications," *Int. J. Inf. Technol.*, vol. 13, no. 3, pp. 829–837, Jun. 2021.

[53] Y. Hu, A. Luo, J. Wang, and F. Wang, "Voltage regulation and power management for wireless flow sensor node self-powered by energy harvester with enhanced reliability," *IEEE Access*, vol. 7, pp. 154836–154843, 2019.

[54] S. Saxena, N. A. El-Taweel, H. E. Farag, and L. S. Hilaire, "Design and field implementation of a multi-agent system for voltage regulation using smart inverters and data distribution service (DDS)," in *Proc. IEEE Electr. Power Energy Conf. (EPEC)*, Toronto, ON, Canada, Oct. 2018, pp. 10–11.

[55] E. J. Okampo, N. Nwulu, and P. N. Bokoro, "Optimal placement and operation of FACTS technologies in a cyber-physical power system: Critical review and future outlook," *Sustainability*, vol. 14, no. 13, p. 7707, Jun. 2022.

[56] Annual Report. (2020). *North Delta Electric Distribution Company*. [Online]. Available: http://www.ndedco.org

[57] J. Tang, D. Cai, C. Yuan, Y. Qiu, X. Deng, and Y. Huang, "Optimal configuration of battery energy storage systems using for rooftop residential photovoltaic to improve voltage profile of distributed network," *J. Eng.*, vol. 2019, no. 16, pp. 728–732, Mar. 2019.

[58] A. Nasri, M. E. H. Golshan, and S. M. S. Nejad, "Optimal planning of dispatchable and non-dispatchable distributed generation units for minimizing distribution system's energy loss using particle swarm optimization," *Int. Trans. Electr. Energy Syst.*, vol. 24, no. 4, pp. 504–519, Apr. 2014.

[59] J. Faiz and B. Siahkolah, "Implementation of a low-power electronic tap-changer in transformers," *IET Electric Power Appl.*, vol. 2, no. 6, pp. 362–373, Nov. 2008.

[60] K. D. E. Kerrouche, E. Lodhi, M. B. Kerrouche, L. Wang, F. Zhu, and G. Xiong, "Modeling and design of the improved D-STATCOM control for power distribution grid," *Social Netw. Appl. Sci.*, vol. 2, no. 9, pp. 1–11, Sep. 2020.

[61] M. Dosoglu, A. B. Arsoy, and U. Guvenc, "Application of STATCOM super capacitor for low-voltage ride-through capability in DFIG based wind farm," *Neural Comput. Appl.*, vol. 28, no. 9, pp. 2665–2674, 2017.

[62] P. P. Biswas, P. N. Suganthan, and G. A. J. Amaratunga, "Optimal power flow solutions incorporating stochastic wind and solar power," *Energy Convers. Manag.*, vol. 148, pp. 1194–1207, Sep. 2017.

[63] A. Soroudi and T. Amraee, "Decision making under uncertainty in energy systems: State of the art," *Renew. Sustain. Energy Rev.*, vol. 28, pp. 376–384, Dec. 2013.

[64] R. Jabbari-Sabet, S.-M. Moghaddas-Tafreshi, and S.-S. Mirhoseini, "Microgrid operation and management using probabilistic reconfiguration and unit commitment," *Int. J. Electr. Power Energy Syst.*, vol. 75, pp. 328–336, Feb. 2016.

[65] B. E. Sedhom, M. M. El-Saadawi, M. S. El Moursi, M. A. Hassan, and A. A. Eladl, "IoT-based optimal demand side management and control scheme for smart microgrid," *Int. J. Electr. Power Energy Syst.*, vol. 127, May 2021, Art. no. 106674.

[66] N. Nikmehr and S. N. Ravadanegh, "Reliability evaluation of multimicrogrids considering optimal operation of small scale energy zones under load-generation uncertainties," *Int. J. Electr. Power Energy Syst.*, vol. 78, pp. 80–87, Jun. 2016.

[67] A. A. Eladl, M. A. Saeed, B. E. Sedhom, and J. M. Guerrero, "IoT technology-based protection scheme for MT-HVDC transmission grids with restoration algorithm using support vector machine," *IEEE Access*, vol. 9, pp. 86268–86284, 2021.

[68] S. Mirjalili and A. Lewis, "The whale optimization algorithm," *Adv. Eng. Softw.*, vol. 95, pp. 51–67, Feb. 2016.

[69] B. Abdollahzadeh, F. S. Gharehchopogh, and S. Mirjalili, "Artificial gorilla troops optimizer: A new nature-inspired metaheuristic algorithm for global optimization problems," *Int. J. Intell. Syst.*, vol. 36, no. 10, pp. 5887–5958, 2021.

[70] A. Y. Hatata, M. A. Essa, and B. E. Sedhom, "Adaptive protection scheme for FREEDM microgrid based on convolutional neural network and gorilla troops optimization technique," *IEEE Access*, vol. 10, pp. 55583–55601, 2022.

AHMED Y. HATATA received the B.S., M.S., and Ph.D. degrees from the Department of Electrical Engineering, Faculty of Engineering, Mansoura University, Egypt, in 2002, 2007, and 2012, respectively. He became an Assistant Professor at Mansoura University, in 2012, and an Associate Professor, in 2019. He is currently working as an Associate Professor with the College of Engineering, Shaqra University, Saudi Arabia. His research interests include the operation, control and protection of distribution systems, power quality, power system optimization, renewable energy sources, micro grids, and smart grids.

EMAN. O. HASAN received the B.Sc., M.Sc., and Ph.D. degrees in electrical engineering from the Faculty of Engineering, Mansoura University, El-Mansoura, Egypt. She is currently an Engineer with North Delta Electricity Distribution Company (NDEDC), Egypt. Her research interests include energy management, power quality, and optimization methods.

MOHAMMED A. ALGHASSAB was born in Ha'il, Saudi Arabia, in 1984. He received the bachelor's degree in electrical engineering from Ha'il University, in 2006, the master's degree from Gannon University, USA, in 2012, and the Ph.D. degree from Oakland University, USA, in 2018. Joining LHPU helped him to acquire real-time experience in the field of controls and renewable energy, where he learned J1939 CAN communication protocol and to build engine control models using MATLAB and SIMULINK. This helped him to calibrate and validate APP and TPS sensors on the engine. He wants to pursue a Powertrain Calibration Engineer career, where he can calibrate engines to improve vehicle drivability and emission. He worked at Saudi Electricity Company in the new program development to check the whole system in the field and maintained the initial problem with experienced engineers. He is currently an Assistant Professor with Shaqra University and an Assistant Head with Vision 2030.

BISHOY E. SEDHOM (Member, IEEE) received the B.Sc. (Hons.), M.Sc., and Ph.D. degrees in electrical engineering from the Faculty of Engineering, Mansoura University, El-Mansoura, Egypt. Currently, he is an Assistant Professor with the Electrical Engineering Department, Mansoura University. His research interests include energy management, microgrid operation and control, power system protection, power quality, the Internet of Things, optimization methods, islanding detection, system restoration, microgrid protection, smart manufacturing, cybersecurity, shipboard microgrids, HVDC protection and control, electric vehicles, and hydrogen generation. He received the Best Ph.D. Thesis Award from Mansoura University, in 2019.

• • •

11922

VOLUME 11, 2023